PETROPHYSICAL ANALYSIS OF TOLANJ-01 WELL, KHUSHALGARH BLOCK A, UPPER INDUS BASIN, PAKISTAN

By

Abdul Ahad

Abdul Hameed

Muhammad Munhim-ur-Rehman

Department of Earth and Environmental Sciences

Bahria University, Islamabad

2019

PETROPHYSICAL ANALYSIS OF TOLANJ-01 WELL, KHUSHALGARH BLOCK A, UPPER INDUS BASIN, PAKISTAN

A thesis submitted to Bahria University, Islamabad in partial fulfillment of the requirement for the degree of BS in Geology

Abdul Ahad

Abdul Hameed

Muhammad Munhim-ur-Rehman

Department of Earth and Environmental Sciences

Bahria University, Islamabad

2019

DEDICATION

We dedicate this research work to our parents who always loved and appreciated us. We thank them for providing us support and encouragement. We are also grateful to our teachers and class fellows who assisted, cooperated and guided us throughout our research work.

ABSTRACT

For the exploration of hydrocarbons, petrophysical analysis has been done in Tolanj-01 well in Khushalgarh block Upper Indus Basin Pakistan. In Tolanj-01 drilling has been done from Kohat Formation of Eocene age up to Samana Suk Formation of Jurassic age. Logging suits including caliper log, spontaneous potential log, spectral gamma ray log, computed gamma ray log, dual laterolog, microspherically focused log, neutron log, density log and sonic log have been run from depth of 7740 ft to 10120 ft. Two zones have been marked from 7980 feet to 8094 feet in Lockhart Formation and 8598 feet to 8682 feet in Hangu Formation respectively, on the basis of calculated petrophysical parameters i.e. low GR log values, high LLd values and neutron-density crossover. Both the marked zones have low volume shale, low effective porosity and low hydrocarbon saturation that is why it is showing low hydrocarbon potential. Identification of lithology and mineralogical composition have been done with the help of M-N, neutron-density, neutron-sonic cross plots and PEF log and it was found that the lithology of Lockhart Formation is limestone having calcite and some dolomite minerals whereas lithology of Hangu Formation is Sandstone. GR log is indicating the lithology of the Lockhart formation is pure limestone at upper part having no organic matter and showing oxidizing environment of deposition, whereas shaly to pure limestone at lower part, having the organic matter and reducing environment of deposition. In Hangu Formation GR log is indicating the lithology of formation is dirty at upper part and pure at the lower part which is marked as hydrocarbon zone.

ACKNOWLEDGEMENTS

ABBREVIATIONS

OGDCL	Oil and Gas Development Company Limited
LMKR	Landmark Resources
DGPC	Directorate General of Petroleum Concession
PEF	Photo-Electric Factor
LLS	Shallow Lateral Log
LLD	Deep Lateral Log
MSFL	Micro-Spherically Focused Log
SP	Spontaneous Potential
B.H.T	Bottom Hole Temperature
Fm	Formation
Vsh	Volume of Shale
GR log	Gamma Ray Log
GR min	Gamma Ray minimum
GR max	Gamma Ray maximum
SGR Log	Spectral Gamma Ray
CGR Log	Composite Gamma Ray Log
ρma	Density of Matrix
ρf	Density of Fluid
Sh	Saturation of Hydrocarbons
Sw	Saturation of Water
Rmfeq	Resistivity of Mud Filtrate Equivalent
T.D	Total Depth

CONTENTS

CHAPTER 1

INTRODUCTION

CHAPTER 2

GENERAL GEOLOGY

CHAPTER 3

PETROPHYSICAL ANALYSIS

FIGURES

TABLES

CHAPTER 1
INTRODUCTION

1.1   General statement

Currently, world energy sector-controlled the economy. The purpose of this to control the political and economic position of the state. Availability and extraction of hydrocarbon directly affect development and prosperity of state (Alger, 1980).

In the oil exploration, the main interest is the identification of porosity and permeability in the formation, thickness, besides its size with a lateral a lateral and vertical extension of the reservoir. All of this information acquires from the well logging by measuring and evaluating the properties of formation (such as physical, chemical, and lithological) (Alger, 1980).

This required information is when interrelated to another information from core analysis, to give its depth, nature, type of fluid, extent, its porosity, permeability, mobility, flow rate, pressure, and many other factors with high precision. The advancement of technology has found their applicability in well logging. The measuring of down-hole data through wire line cable provides the scope of recording great amount of information in data acquisition. Hence data acquisition and interpretation by computer in the well logging has created future new prospect for the exploitation of the hydrocarbons. Geophysical well logging played a main role in discovery and development of hydrocarbons. Rock cuttings tells the present lithology and the rock nature by the drilling process but not sure about their occurrence. Core drilling helps but it is extremely expensive and has incomplete information about the formation fluids. Hence, the well logs are necessary for complete evaluation of formation.

Well's productivity of reservoir contains oil and gas depending upon petrophysical properties, mainly consist of different components like rock matrix and interconnected pore spaces varying in dimension in sandstone(sub-microns), carbonates rock(centimeter). (Levorsen, 1967).

Accurate estimation of these petrophysical properties are essential for economic viability for the development of the reservoir. Lately, the well logging technology has led

to more developments in data acquisition and interpretation techniques due to advancement of technology in this field. In the west, logging companies are equipped with highly advanced logging systems.

Petrophysical analysis of rock samples determines only one property at same time. This can characterize the reservoir consisting of the rock layer determine the volume of hydrocarbons, their drilling plan and methods of production. Reservoir capacity calculations or hydrocarbons initially in place (HIIP) is directly affected by the porosity, the evolution producing reservoir is determined by the permeability. Lithology determines many factors such as environment of deposition, age, boundary between reservoir and non-reservoir etc. The estimation of resources related to the potential phase directly affected by the Fluid saturation.

1.2   Study area

Kohat Plateau is the northern most element of the Indus basin. Kohat Plateau is bounded on the north by the Kalachitta mountain ranges through a series of faults. In the southern side, salt range composite orocline is present. On its western limit Kurram thrust fault marks its boundary. The Kohat Depression from the Sulaiman Fold Belt is separated by the Pezu wrench fault

In 26/11/1991 at Kohat the well of AMOCO was drilled in Khushalgarh block A, Kohat Plateau Upper Indus basin.

Nearby Tolanj-01 lies Sumari-01, and Kahi-01 well on the western side and Dakhni-01 well on the eastern side.

1.3   Location of the study area

Tolanj-01 well is located about 158 km southwest of Islamabad. Tolanj-01 well lies in Khushalgarh block A. Khushalgarh block lies in Kohat/Peshawar district, Upper Indus Basin, Pakistan. The latitude and longitude of Tolanj-01 well are 33⁰33'42''N and 71⁰42'50''E (Fig. 1.1).
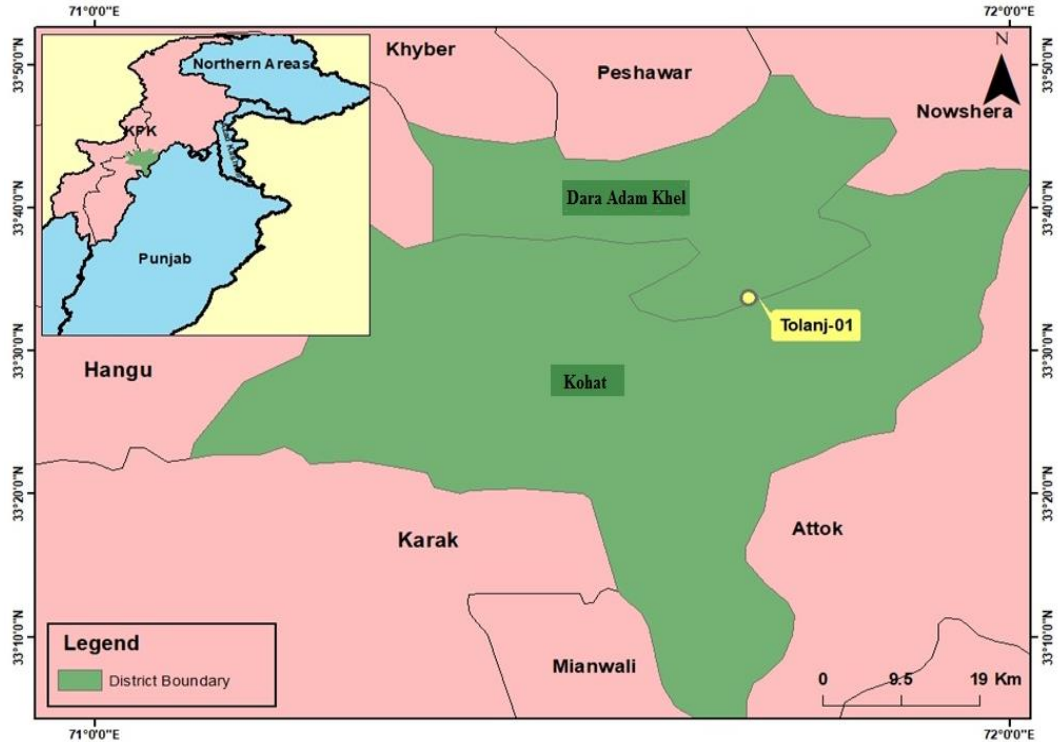
Figure 1.1. Map showing location of Tolanj-01 well.

1.4   Topography and climate

Topographically, it is a plain area with scattered dunes of moderate relief. Hot arid condition dominate for most of the year and area experiences less rainfall. During summer season the temperature ranges between 30-50ºC. Vegetation is widely spread along the sub-tropical green shrubs (Bender and Raza, 1989).

1.5   Objectives of the study

Followings are the objectives:

1)   To determine the petrophysical parameters of Tolanj-01.

2)   To identify the lithological and mineralogical composition.

3)   To delineate the hydrocarbon potential of Tolanj-01

1.6   Data required

All log suits are required to carry out petrophysical analysis of Tolanj-01 well.

These log suits are as follows:

1)   Lithological logs

2)   Fluid indicator logs

3)   Porosity logs

1.7   Methodology

Petrophysical analysis methodology adopted is shown in figure 1.2

```
┌─────────────────────────────────────────────────────┐
│                   QUALITY CHECK                      │
└─────────────────────────────────────────────────────┘
                          ↓
┌─────────────────────────────────────────────────────┐
│                  RAW  LOG  CURVES                    │
└─────────────────────────────────────────────────────┘
                          ↓
┌─────────────────────────────────────────────────────┐
│              MARKING ZONE OF INTEREST                │
└─────────────────────────────────────────────────────┘
                          ↓
┌─────────────────────────────────────────────────────┐
│           CALCULATION OF VOLUME OF SHALE             │
└─────────────────────────────────────────────────────┘
                          ↓
┌─────────────────────────────────────────────────────┐
│               CALCULATION OF POROSITY                │
└─────────────────────────────────────────────────────┘
                          ↓
┌─────────────────────────────────────────────────────┐
│          CALCULATION OF RESISTIVITY OF WATER         │
└─────────────────────────────────────────────────────┘
                          ↓
┌─────────────────────────────────────────────────────┐
│          CALCULATION OF SATURATION OF WATER          │
└─────────────────────────────────────────────────────┘
                          ↓
┌─────────────────────────────────────────────────────┐
│       CALCULATION OF SATURATION OF HYDROCARBON       │
└─────────────────────────────────────────────────────┘
                          ↓
┌─────────────────────────────────────────────────────┐
│      LITHOLOGICAL AND MINERALOGICAL IDENTIFICATION   │
└─────────────────────────────────────────────────────┘
                          ↓
┌─────────────────────────────────────────────────────┐
│                    CONCLUSIONS                       │
└─────────────────────────────────────────────────────┘
```
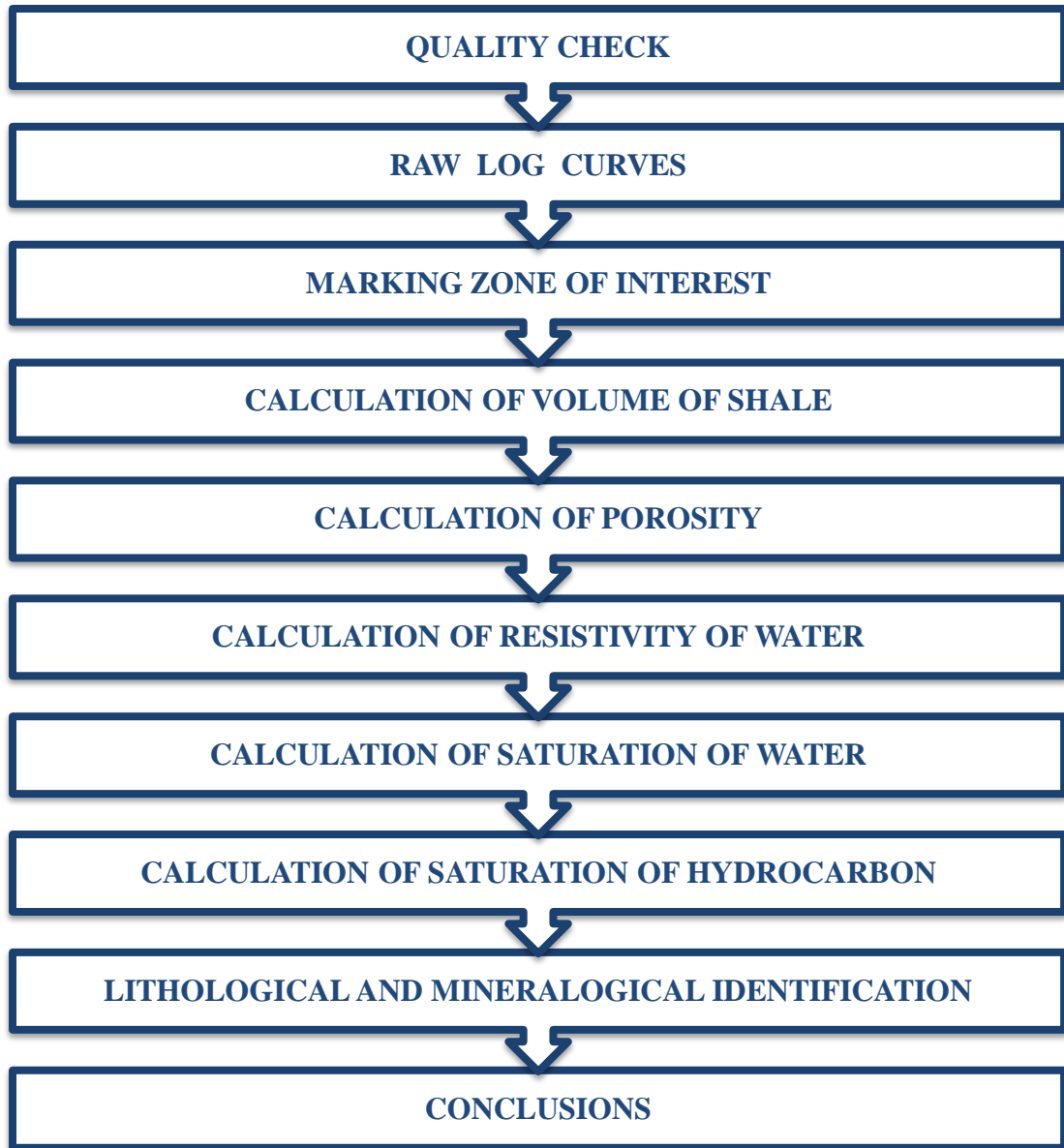
Figure 1.2. Flow chart for petrophysical analysis.

CHAPTER 2
GENERAL GEOLOGY

2.1   Regional geologic settings

Pakistan is section off into two major sedimentary basins namely Indus and Balochistan Basins, which transform drastically after experiences distinctive geological deformation through various stages and eventually firmed or welled together at a period of the Cretaceous / Paleocene age. Kakar-Khorason also referred as Pishin Basin.

Pishin Basin has been discovered, for main part of its development possessing its own Geological history. This basin is classified as Median Basin due to the collision between Indian and Eurasian plates (Raza et al, 1989)

2.2   Indus basin

There are two major Basins in Pakistan Indus Basin and Baluchistan Basin. Indus Basin is the largest Basin of Pakistan which is classified in following Sub-Basins.

1)   Upper Indus Basin

2)   Central Indus Basin

3)   Southern Indus Basin

Sarghoda high divides the Indus basin into two parts, one is named as Upper Indus and Central Indus Basins. Jaccobabad high gives the line of division to Central and Southern Basins. Upper Indus Basin gives supplementary divisions in the form of the Kohat and Potwar Sub-Basins. (Raza et al, 1989)

In the tectonics plates, the compressional regimes cause the division of Upper Midlle and Lower Indus basins. In the west, fold and thrust belts of Kirthar and Sulaiman Ranges, Kohat-Potwar Plateau runs to the north, Indian Craton to the east and Indus basins runs in the prevailing trend of north-south.

2.3   Kohat Sub-basin

It is one of the subdivisions of upper Indus basin. The Salt Range having width of 85 km with the length of 200 km situated in westward extension of Sub Himalaya. Kohat Plateau comprise of valley with low roll hills, Main Boundary Thrust (MBT) lying at north dipping orientation (Fig. 2.1)

At higher level of the Kohat basin, salt present apart from Potwar basin and allotted to southward direction and experienced less movement in northward within the sedimentary basin. This basin is bounded by Parachinar Murree fault, kurram fault, Surghar and Jhelum fault on the north, south, east, west respectively and it is an onshore basin (Kazmi and Jan, 1997).
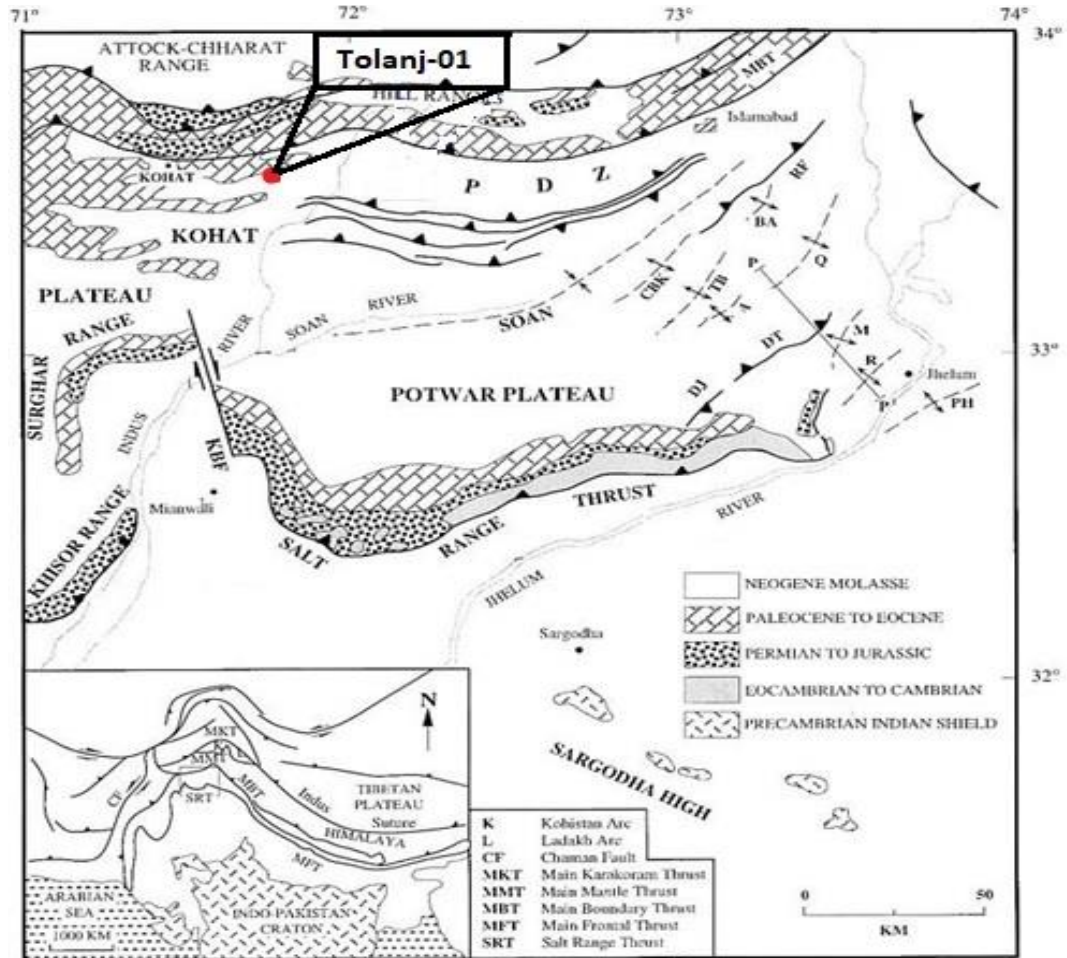
Figure 2.1. Regional stratigraphy and regional tectonics of NPDZ showing location of Tolanj-01 well (Kazmi and Jan, 1997).

In the tectonically restricted basin, Kohat Plateau with deposited rocks is consisting of Eocene and younger sedimentary rocks. In southern part of the plateau, the evaporites of Eocene sequence are limited. Folds of Kohat Plateau in the southern part trending in East West direction, reverse faults frequently dipping in north and south. Tectonically Kohat basin is complicated area where large numbers of faults both normal and thrust faults are present due to the steeper dips and asymmetrical structures. In northern Pakistan, Kohat-Potwar Plateau is the most complex tectonic zone (Kazmi and Jan, 1997).

In Kohat plateau, northern area is deformed more as compared to southern and southeastern parts. Kalachitta Hills bound Kohat-Potwar Plateau from north, whereas to the south the Salt Range marks boundary to the west. Kohat-Potwar Plateau in the Potwar region is separated by Indus River trending east and West respectively (Kazmi and Jan, 1997).

2.4   Tectonic framework
2.4.1   Introduction

Indian plate under thrusting to the northward beneath the Eurasia continues to create the active features on the northern fringes of the Indian Craton since major collision begins in Eocene age. In the Himalayan foreland of Pakistan, thin skinned tectonic features are developing in the Salt Range and Potwar Plateau (SR/PP) as a wedge of sediments is being contracted and thrusted southward along a decollement in Eocambrian evaporite bed. The NPDZ can be divided into two parts. The western NPDZ is an emergent foreland folds and thrust front while the eastern NPDZ is a buried one (Jaswal et al., 1997), Soan syncline divided these two, eastern and western deformed zones.

2.4.2   General geology and tectonics

The northern part of Pakistan has been deformed tectonically as a result of continent-continent collision of the Indo-Eurasian Plates. After continents collision, a SE to NW rotational movement of the continent resulted in structural changes occurring in the area (Fig 2.2). This collision and later rotational movement have resulted in a WNW-ESE

trend of thrust tectonics in the Potwar area (Paracha, 2000). Region between Sargodha high and MBT forms the northern zone, which contains the Kohat-Potwar plateau, the Bannu basin, the Cis, Trans Indus Salt Range and the northern Punjab monocline (Khan et al., 1986).
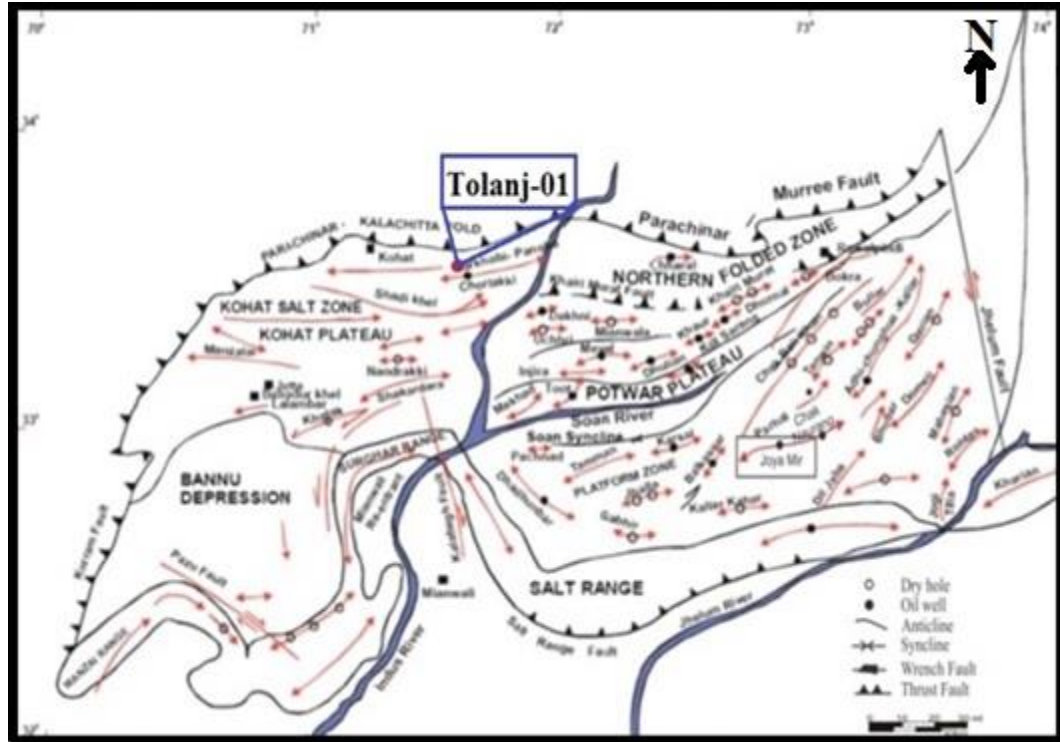
Figure 2.2. Structural and geological map of Kohat-Potwar sub basin showing location of Tolanj-01 (Khan et al., 1986).

On northern Pakistan, Kohat-Potwar basin is situated with the latitude 32º and 34º and longitude 70º and 74º, this offshore basin bounded by Parachinar-Murree to the north fault, by Kurram fault to west, by Salt Ranges and Surghar to the south and Jhelum fault to the east. Collision of the Indian-Eurasian plate cause the deformation of Kohat-Potwar basin. Indus River divides the Kohat basin to the west and Potwar basin to the east.

The northern part of Kohat-Potwar Plateau also referred to as the NPDZ, lies between the Main Boundary Thrust and Soan syncline (Fig. 2.2.). It is more intensely

deformed then the southern limbs, southern Potwar and Salt Range. Mostly E-W trending tight and complex folds are seen with their southern limbs overturned with steep angle faults. Kohat basin is tectonically complex area and it is a tilted plateau where moderate to steeper dips and asymmetrical structures resulted in a large number of thrusts/normal faults. In northern Pakistan the Kohat Basin area of the Kohat-Potwar Plateau is the most complicated tectonic zone. The magnitude of the tectonic vector forces effect is more intensive in the western part as compared to the eastern part, due to which the tectonic rotational activities have occurred (Kazmi and Jan, 1997).

Thus, the tectonic potential is greater in the western part compare to the eastern part of the Kohat-Potwar Sub-basin.

2.4.3   General stratigraphy

Depositional history of Kohat-Potwar Fold Belts goes back in Precambrian because of the deposition of sediments of Jhelum Group and Salt Range Formation (Table 2.1). Upper Cambrian, Ordovician, Silurian, Devonian or Carboniferous sediments are not present in this basin due to erosion and/or non-deposition (Shah, 1977).

Table 2.1. Generalized stratigraphy of Kohat Sub-basin (Kadri, 1995)

Age	Formation			Lithology		
Pliocene	Dhok Pathan			Sandstone		
	Nagri			Sandstone, clay		
	Chinji			Sandstone, clay		
Miocene	Kamlial			Sandstone		
	Murree			Sandstone, clay		
Eocene	Kohat			Limestone		
	Mami khel			Clay		
	Shekhan		Jatta	Limestone		Gypsum
	Panoba	Bahadurkhel	Sakesar	Shale	Salt	Limestone
Paleocene	Patala			Shale, Limestone		
	Lockhart			Limestone		
	Hangu			Sandstone		
Cretaceous	Darsamand			Limestone		
	Lumshiwal			Sandstone, Siltstone		
	Chichali			Siltstone, Clay		
Jurassic	Samanasuk			Limestone		
	Datta			Sandstone, shale		
Triassic	Permian and Triassic rocks. Undivided					
Permian						
Precambrian	Attock Slate			Slate, Quartzitic sandstone		
	Pitao Ghar			Sandstone, Shale		

2.5   Stratigraphy of Kohat sub-basin

There are several disconformities in the fold belt of Mesozoic strata that is overlying the Permian strata which is incomplete. In the east, upper Permian to Mesozoic section is almost removed due to tilting, uplifting and erosion event of late Cretaceous to Paleocene represented by major unconformities at the base of Paleocene. Clastic sediments of the Hangu Formation in the Paleocene Era was resumed on passive margin of Indian plate. Shallow marine and lagoonal strata of Lower to Middle Eocene are the last deposits of marine sediments in the Kohat-potwar Fold Belts. There is disconformity in the Oligocene that is why there is no deposition occurred in Oligocene. There is a major unconformity which separates the continental strata Neogene deposits from underlying Paleogene strata (Shah, 1977).

2.5.1   Kohat Formation

The name Kohat Shales and Kohat Limestone is used by Eames in 1952 and has been formulized by the Stratigraphic Committee of Pakistan (Fatmi, 1977) as Kohat Formation. Meissner et al (1974) divides the formation into 3 members i.e. Kaladhand Members as lower one, Sadkal Member as upper one while the third one Habib Rahi Member is the lower member of Kirthar Formation of the Sulaiman Province, exposed here in Kohat area. The formation is composed of limestone and intebedded shales.

The Kaladhand member is mainly composed of light grey, thin bedded limestone with interclation of shale in its lower parts while the upper Sadkal member is composed of calcareous, greenish grey shale and grey limestone. The age of the formation is Eocene (Shah, 1977).

2.5.2   Mami khel Clay

The author proposed the name as Mami Khel Clay to this formation. In April, 1964 the Stratigraphy committee of Pakistan recognized its stratigraphic name given as a Mami Khel Clay. At the type locality of Miami Khel Clay, the thickness of the beds is 406 feet, color of the clay is brownish red to red which is soft, calcareous and silty. The Samples taken or Studied at this area found no fossils, however, 16 miles to north of the Miami khel

in the Chilli Bagh Section samples taken out from the same formation contains the fossils of the Early Eocene Foraminifera, Eponides, Cibinides and Lokhartia (huntil) were found (Shah, 1977).

2.5.3 Shekhan Limestone

In 1930, Davies named the Shekhan Limestone on the basis of the outcrop in the location of Shekhan Nala, east town of the Kohat. Later on, in 1952, Shekhan Limestone was subdivided by Eames into the four units such as; Lower Shekhan Limesone, Middle Shekhan Limesone, Upper Shekhan Limesone and Gypsiferous Bed. In the regional Geological Settings, the author did not accept these subdivisions of this formation.

The thickness of the Shekhan Limestone is about 235 feet. It comprises of the Limestone containing Shale partings to the bottom 90 feet. The highest subsequent contains dusky-fossiliferous shale with thickness of 50 feet. The topmost having thickness of 95 feet limestone comprising of thin layers of gypsum. Limestone color is from yellowish grey-to-grey, massive bed, nodular, argillaceous, containing Foraminifera. The contact of this formation with overlying beds is conformable with Eocene beds (Shah, 1977).

2.5.4 Panoba shale

In 1952, Eames named the Panoba Shales and also stratigraphy committee of Pakistan suggest its name as Panoba shale. The type locality of the Eames's section is located on the east of Kohat quadrangle near by the Panoba Village. At the Panoba, shale thickness is about 335 feet having color greenish-grey to light olive. At Uch Bazaar and Tarkhobi, Panoba Shale has also been measured and exposed somewhere near cores of anticlines which are eroded. The thickness of the formation varies from one section to another section, at the Uch Bazar thickness of the section is about 525 feet. The fossils of the foraminifera have been identified of early Eocene age. The upper part of the Panoba Shale is confirmable with overlying beds of the Eocene age excluding west side of the quadrangle (Shah, 1977).

2.5.5   Patala Formation

In the surghar ranges, Davies, 1930 gave a rock name to the sequence of Patala Nala, on that basis of that identification Patala Formation attain its name from the Patala Shales. After that, Tarkhobi shales of Eames (1952) was correlated with Patala Shales in the area of Kohat but, due to significant difference of lithology, suggested the name as Tarkhobi Formation. In 1964, the stratigraphy of Pakistan decided or agreed to recognize the formation with their prior name as Patala in place of the Tarkhobi.

At section of Mazari tang, Patala formation exposes with a thickness of 604 feet. The top part of the Patala formation having faults which are in contact with Crataceous Limestone. Subsequent unit, comprises of thick bedded nodular limestone, with grey, Brownish grey or dark-grey finely crystalline to medium crystalline. This highest unit is measure with a thickness of the 225 feet. The third unit is 102 feet thick, comprises of the siltiest thin bedded limestone which is highly fossiliferous. The upper unit comprises of the fossiliferous limestone that is finely and hard crystalline light to dark-brownish-grey with a thickness of the 139 feet. The fresh samples give strong pungent smell. The age of exposed Patala formation at Mazari Tang section is Paleocene (Shah, 1977).

2.5.6   Lockhart Formation

Lockhart Formation was named by Davies, 1930 from location near Fort Lockhart. In every section the Lockhart Formation contains fairly even lithology varying in thickness. At Uch Bazaar, the thickness of the limestone is 150 feet having a blocky appearance cause of the joints with Attributes of massive, hard, dark grey to black and finely crystalline. In the Tarkhobi section, the Lockhartia Formation exposed a thickness of the 453 feet with invisible base due to total thickness is undetermined or unmeasured. In 1952 Eames, suggested the name as Tarkhobi limestone due to exposed of thick limestone at the Takhobi limestone. The 'lockhartia' name gets precession to the Tarkhobi. The fresh samples give strong pungent smell (Shah, 1977).

2.5.7 Hangu Formation

The name of Hangu sandstone was suggested by Davies in 1930 that is overlying Upper Cretaceous limestone in the north of the Hangu region. In the northward and eastward of Kohat quadrangle area consisting sandstone converted into the limestone and shales. The authors observed that lateral changes in facies of the Hangu sandstone to limestone to shale, and replaced the name from Hangu sandstone to Hangu formation also to comprise lateral changes in lithology. In April 1964, SCOP recognized Hangu Formation by replacing with the name Hangu Sandstone.

At Uch Bazaar section, Hnagu formation comprises sandstone of about 215 feet, that is white and stained rusty, round-medium size quartz grains and small limonitic nodules are present. This section includes cross bedding also comprises conglomerate lenses that contains quartz in sandstone and cherts pebbles in minor amount having diameter one quarter to one-half of an inch. In 1930, Davies discussed yellow fossiliferous clay at the top of Hangu formation (2 to 20 feet), which he named as Hangu shale that was not seen at the Uch Bazaar (Shah, 1977).

The contact of Hangu formation are conformable with the overlying strata of Lockhart Formation.

2.5.8 Darsamand Formation

The name Darsamand Formation was suggested on basis of the type locality of Darsamand, which is located upto 18 miles to the west of Kohat in Parachinar quadrangle. The authors have also been accepted this unit at Kohat in the sections of Marai Bala, Mazari Tang, and Uch Bazaar.

At Marai Tang, limestone thickness is 400 feet which is explained in three units. The Lower unit with the thickness of 50 feet comprises of the brownish-grey hard thick bedded limestone (nearly 10 ft thick bed). The Middle Unit have thickness of 270 feet consisting of light-dark grey dense hard thin bedded limestone (i.e. 3 inches to 1 ft). It also comprises shale partings and gives break with a conchoidal fracture. The Upper unit with a thickness of 80 feet is transitional with Paleocene beds which is overlying. Generally, Darsamand Formation is forming a slope. The base of unit is sandy, glauconitic, and

fossiliferous (Kazmi and Jan, 1997).

The Makarwal area of the Surghar Ranges does not contain Darsamand Formation. However, Lumshiwal Sandstone of the lower Cretaceous have contact with overlying rocks of Paleocene age. The deposition of Darsamand Formation was not occurred in the area of Surghar Range after the deposition of the Lumshiwal sandstone, might be due to the experience of tectonic uplifting (Kazmi and Jan, 1977).

2.5.9 Lumshiwal Formation

The name Lumshiwal Formation was suggested by the Gee (1989) in the Salt Range. After that, Strarigraphy committee changed the name due to distinguishable lithologies present in that area besides type locality. Authors suggested correlation with the Khadimak Sandstone in the Parachinar quadrangle.

At the Marai Bala, thickness of the Lumshiwal Formation is 450 feet, commonly white in colour while stained brown in places, mostly consisting of the very hard quartzite sandstone. It is fine to medium grained, nearly about the thickness of 6 feet. Generally, beds are break into large blocks by the incision of two sets of well-developed joints. The top thickness of 20 feet is comprises of carbonaceous shale which black in color and sandstone having brownish-green color and medium grain in size. At the location of Marai Bala, Lumshiwal Sandstone has unconformable contact with cretaceous rocks which are overlying which are rich of limonitic fossil casts.

At the Mazari Tang section, thickness of the Lumshiwal Formation is 224 feet which is commonly light brown to white and medium granied sandstone. Thickness of the strata is 38 feet which is well sorted, hard and having composition of quartz grains. At formation top, a 19-feet-thick transitional zone is present which is overlying Upper Cretaceous Darsamand Formation (Kadri, 1995).

2.5.10 Samanasuk Formation

The name Samanasuk Formation was derived from Samana Range by Davies (1930). It consists of mainly limestone with minor shale. Fatmi (1977) reported middle Callovian fauna (brachiopods, bivalves, gastropods, ammonoids and crinoids) from the uppermost part. The ammonoids include Reineckeia, Obtusicostites, Obuckmani, Hubertoceras and Kinkeliniceras. The brachiopods include Somalirhynchia nobelis. The bivalves include Homomya, Pecten, and Tellurimya tellaris. From Samana Range Belemnopsis grantana and Kala Chitta (Jhallar and Chak Dalla) bivalves include Protocardia grandidieri, Eomiodon indicus and Corbula lyrata (Fatmi, 1977). Latif (1969) reported following fauna from Hazara such as Stylina, Corbula, eomiodon, Gervillea, Lima, Lucina, Nucula, Nerinen, Protocardia, Pygurus (Kazmi and Jan, 1997).

Malkani (2007a, 2008a) reported first time in Indo-Pakistan the titanosauriforms/titanosaurs trackways confronted by a running theropod. The two track ways of small theropod meets/overlap/converge with each other and then become diverge showing mating/fighting. All this fauna indicates Middle Jurassic age (Kazmi and Jan, 1997).

2.6   Borehole stratigraphy

Tolanj-01 well was drilled with the total depth of 10167 feet and the last encountered formation is Samana Suk with the depth of 9815 feet (Table 2.2).

Table 2.2. Borehole stratigraphy of well.

Formation	Age	Formation Top (ft.)	Formation Thickness (ft.)
Kohat	Eocene	0.00	385.00
Mami khel	Eocene	385.00	245.00
Shekhan	Eocene	630.00	245.00
Mami khel	Eocene	875.00	655.00
Shekhan	Eocene	1530.00	1780.00
Mami khel	Eocene	3310.00	234.00
Shekhan	Eocene	3544.00	516.00
Panoba	Eocene	4060.00	450.00
Patala	Paleocene	4510.00	3470.00
Lockhart	Paleocene	7980.00	412.00
Hangu	Paleocene	8392.00	293.00
Darsamand	Cretaceous	8685.00	431.00
Lumshiwal	Early Cretaceous	9116.00	700.00
Samana suk	Middle Jurassic	9816.00	351.00

CHAPTER 3
PETROPHYSICAL ANALYSIS

Petrophysical analysis is performed to describe the hydrocarbon potential in a bore hole and performed by using different log curves that are procured by wire line logging. For the estimation of the hydrocarbon potential saturation of water and hydrocarbon, their porosity, and the volume of the shale and sand are calculated of an interested zone.

3.1   Quality check of logs

Logging data of Tolanj-01 well is not of good quality because caliper log is showing that borehole is over-gauge for most of the depth. Overall logs are good and readable. However, at certain depth the log data is found to be affected by poor borehole conditions.

3.2   Log trend of Tolanj-01

In track 01 caliper, size of bit, SGR, CGR and SP logs are presented. Caliper log shows that hole remained almost over gauged for most of the depth in Lockhart Formation as shown in figure 3.1 and under gauged for most of the depth in Hangu Formation as shown in figure 3.2. Large washouts can be seen along certain depths. At certain depths very high values are observed. SP log curve shows little deflection. Overall positive SP log trend is observed.

In track 02, readings are plotted on logarithmic scale which is resistivity log. Resistivity curves showed deviations. Lockhart Formation mostly separation was presented between LLD, LLS and MSFL curves and remained towards the lower side of the scale and in Hangu Formation no separation was present between LLD, LLS and MSFL curves and remained towards the higher side of the scale.

In track 03 sonic, neutron and density logs are run. For Lockhart Formation, where readings of neutron and density logs were not reliable due to rugosity sonic log was used for the calculation of porosity and for Hangu Formation, readings of neutron and density were reliable.
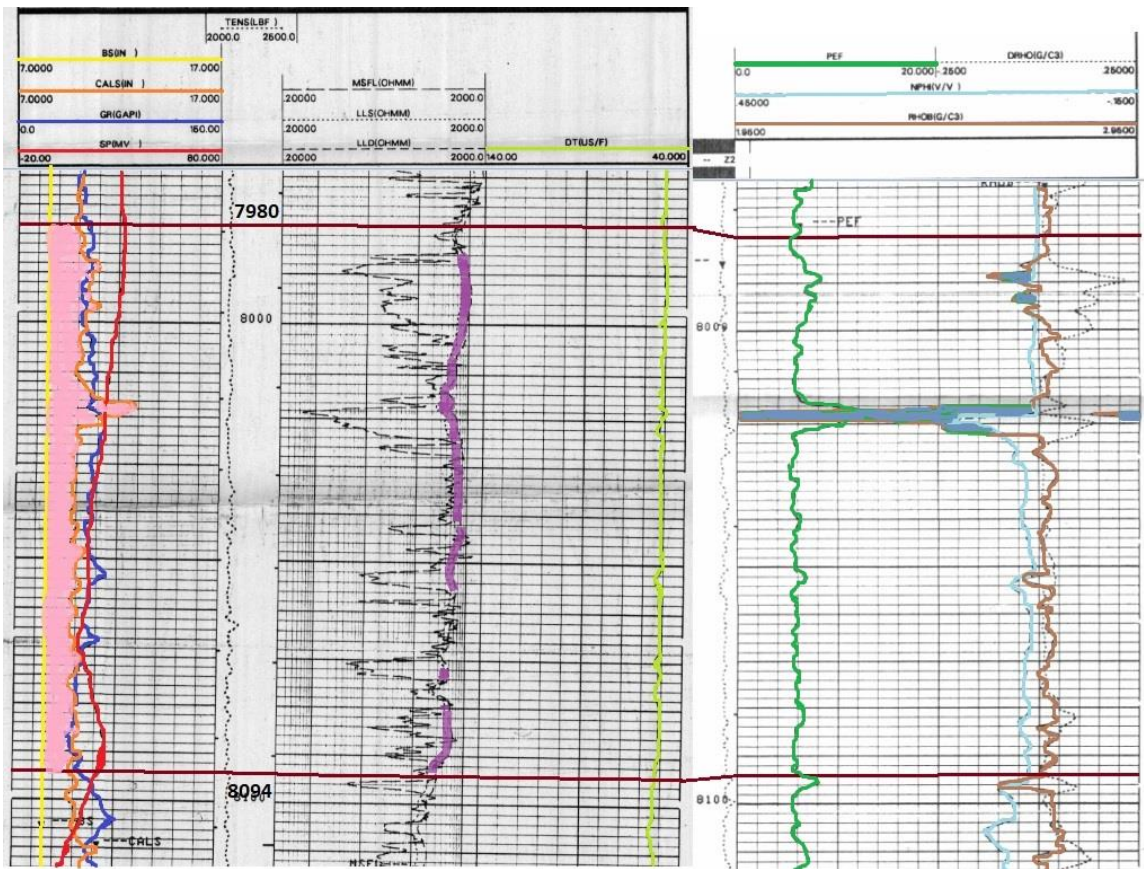
Figure 3.1. Log data showing zone of interest (7980-8094ft.) in Lockhart Formation. Track-01 on left having GR, SP, Bit size and Caliper logs. Track-02 in centre having MSFL, LLs and LLd logs. Track-03 on right having Formation density and neutron porosity logs. (Rugosity=pink, LLd-LLs separation=purple, neutron-density pseudo crossovers=green)

Figure 3.2. Log data showing zone of interest (8598-8682ft.) in Hangu Formation. Track-01 on left having GR, SP, Bit size and Caliper logs. Track-02 in centre having MSFL, LLs and LLd logs. Track-03 on right having Formation density and neutron porosity logs. (Rugosity=pink, LLd-LLs separation=purple, neutron-density pseudo crossovers=green)

3.3   Zones of interest

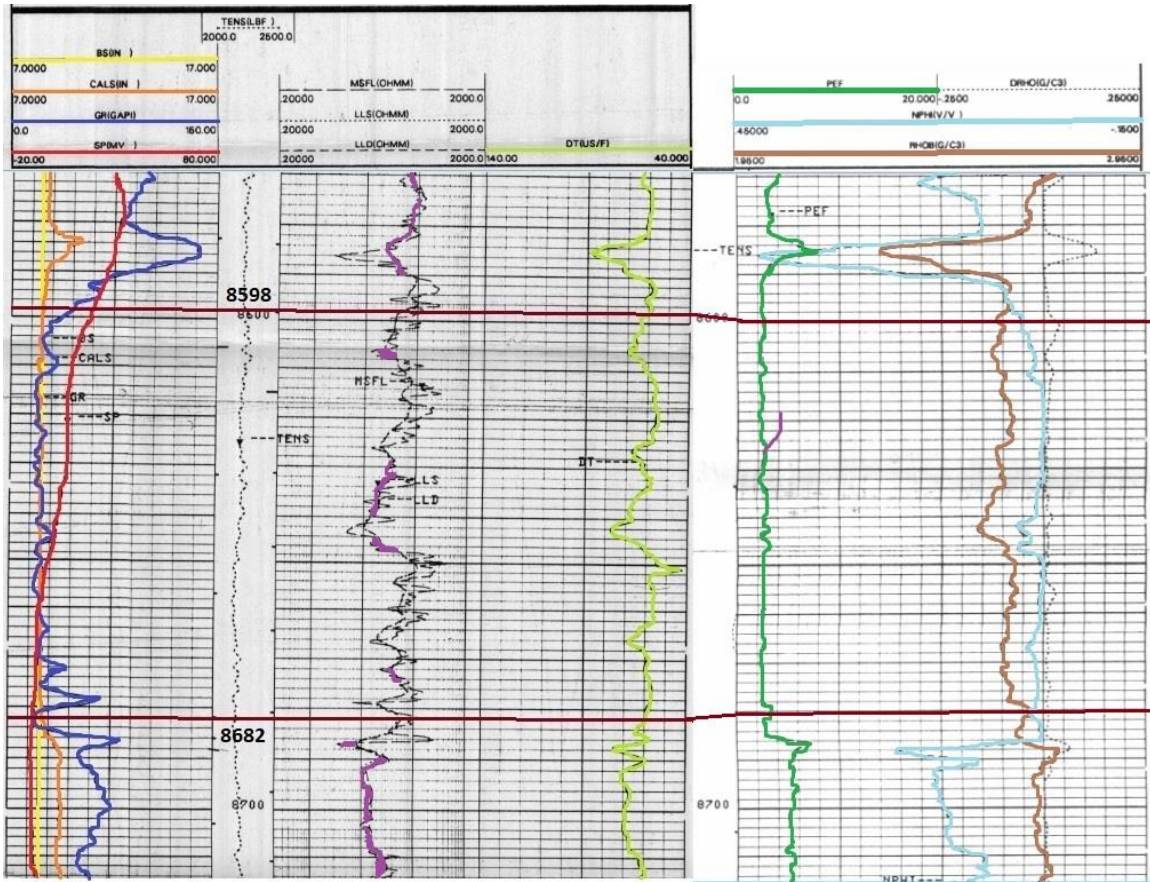Two zones have been marked from 7980 feet to 8094 feet (Table 3.1 and Fig 3.1) and 8598 feet to 8682 feet (Table 3.2 and Fig 3.2) in Lockhart Formation and Hangu Formation respectively, on the basis of low gamma ray values, LLd and LLs separation.

Table 3.1. Zone of interest in Lockhart Formation.

Formation	Starting depth (ft.)	Ending depth (ft.)	Thickness (ft.)
Lockhart	7980	8094	114

Table 3.2. Zone of interest in Hangu Formation.

Formation	Starting depth (ft.)	Ending depth (ft.)	Thickness (ft.)
Hangu	8598	8682	84

3.4   Petrophysical analysis of Tolanj-01

3.4.1   Lockhart Formation

In track-01 minimum CGR log value can be seen in this zone showing the presence of clay free lithology. The average CGR value was around 14 API. The caliper log shows that hole is gauged throughout this zone.

In track-02 there is no such separation between LLD and LLS as shown in figure 3.1, but LLD values are high.

In track-03 there is no such neutron-density crossovers can be seen. As neutron-density crossovers formed where gas zone present and, in this zone, there is no gas present that is why no such neutron-density crossovers can be seen.

3.4.1.1 Volume of shale (Vsh)

It is defined as a quantitative measure of dirtiness in the interested zone, calculated by GR log. Increasing value of gamma ray log represents high radioactive content, showing dirtiness in the lithology. On the other hand, decreasing value of gamma ray log represents clean lithology, showing absence or low concentration of radioactive content.

The Vsh is estimated using CGR log. It is calculated by the following equation.

$$V_{sh} = \frac{CGR_{log} - CGR_{min}}{CGR_{max} - CGR_{min}}$$

Figure 3.3 is representing the relationship between Vsh and Vclean in the zone of interest of Lockhart Formation. It is showing fluctuating trend. Vsh and Vclean showing mirror trend of each other. Maximum value of Vsh is 34% observed at 8054 feet depth and value of Vsh is zero at minimum level observed at 8086 feet and 8088 feet depth. The average value of Vsh is 17.3%. Overall it is showing clean zone.
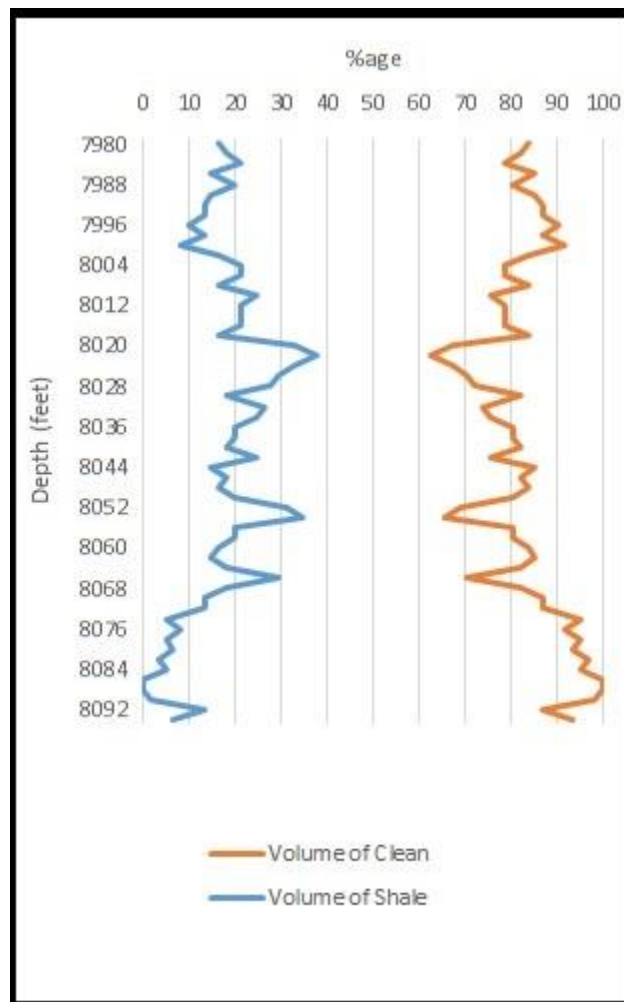
Figure 3.3. Volume of shale and volume of clean in Lockhart Formation.

3.4.1.2 Sonic porosity

As rugosity is observed in the hole due to which the readings of neutron and density logs are not reliable therefore, porosity is calculated through sonic log. Figure 3.4 is representing relationship between average porosity and Vsh in the interested zone with the fluctuating trend of sonic porosity. The average value of sonic porosity is 2.61%.
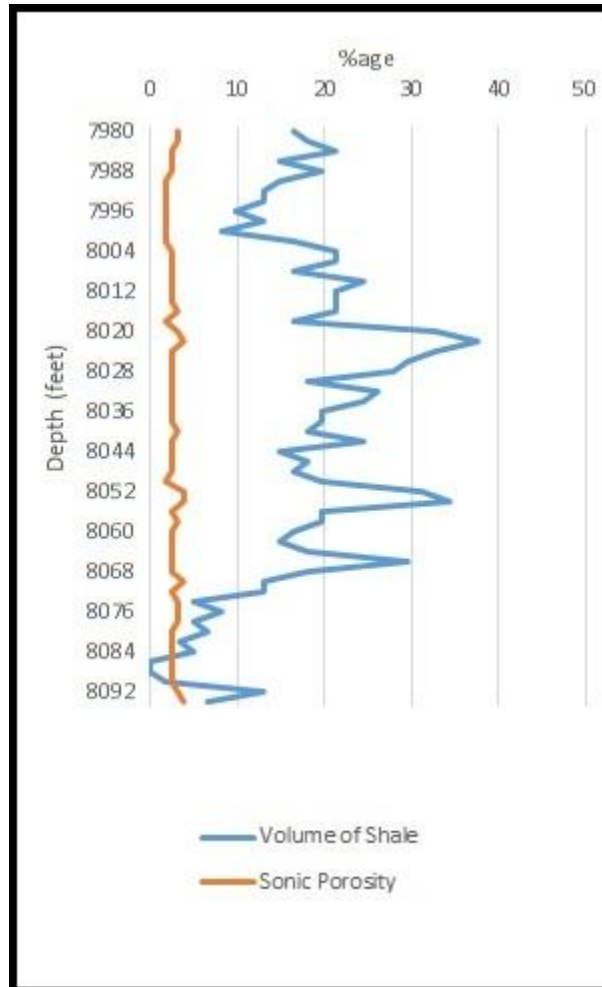
Figure 3.4. Relationship of volume of shale and sonic porosity in Lockhart Formation.

3.4.1.3 Effective porosity

Effective porosity is the total porosity less the fraction of the pore space occupied by shale or clay. In very clean sands, total porosity is equal to effective porosity. It represents pore spaces that contains hydrocarbon and non-clay water.

Figure 3.5 is representing the relationship between effective porosity and Vsh in the interested zone with the same trend as of the sonic porosity (Fig 3.4). The average value of effective porosity is 2.14%.
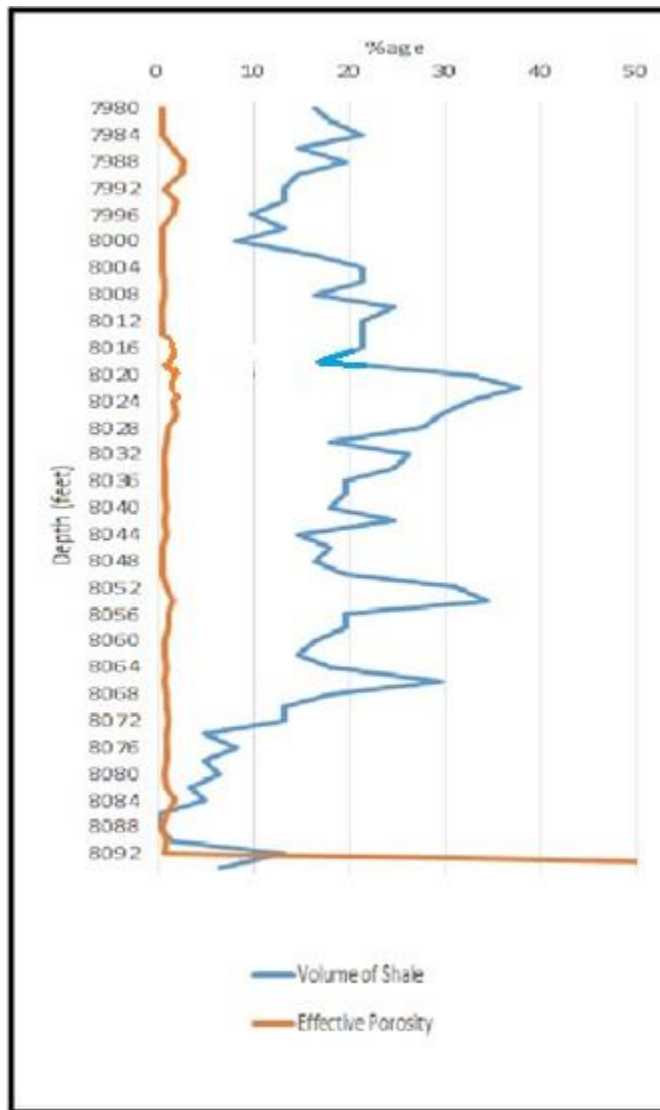
Figure 3.5. Relationship of volume of shale and effective porosity in Lockhart Formation

3.4.1.4 Relationship between sonic porosity, effective porosity and volume of shale

Figure 3.6 is representing relationship between sonic porosity, effective porosity and Vsh in the interested zone. Where Vsh is low, the sonic porosity and effective porosity are equal. It is also evident from the figure that where, Vsh is high, the sonic porosity is greater than the effective porosity due to dirtiness of the lithology.

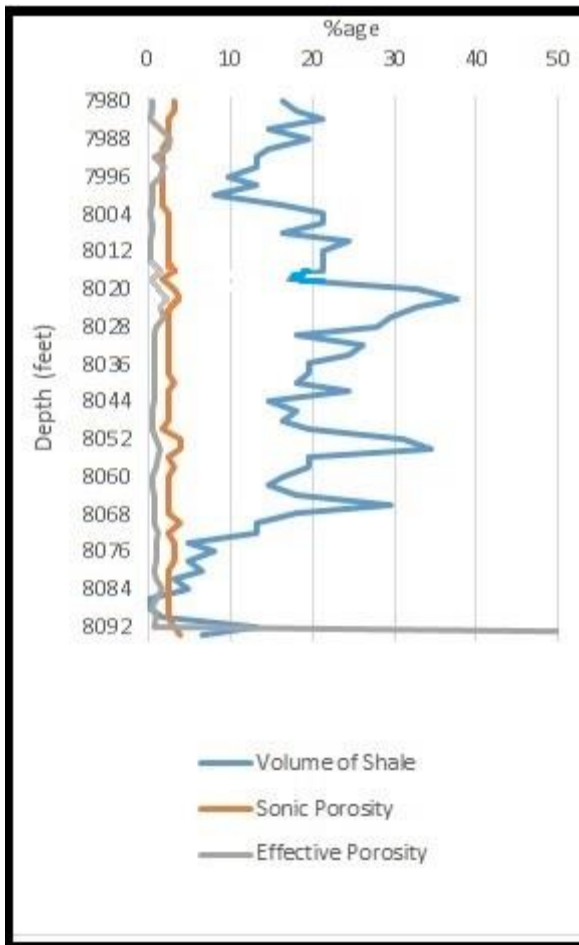

Figure 3.6. Relationship of volume of shale, sonic and effective porosity in Lockhart Formation

3.4.1.5 Resistivity of Water

Water resistivity is an acute parameter for the determination of water saturation. We calculate Rw from Gen-9 and SP chart also Rw computed from SP method equal to 0.023 ohm.m.

3.4.1.6 Saturation of water and hydrocarbons

Hydrocarbon saturation accounts for the percentage of pore fraction that contains hydrocarbon. Water saturation gives the indication of hydrocarbon presence in the reservoir. Low water saturation indicates high hydrocarbon saturation and 100% Sw indicates hydrocarbons are absent in the interval. Analysis of Tolanj-01 well, water saturation calculated by using Archie Equation and Indonesian Equation.

1) **Archie Equation**

$$Sw = \sqrt{((Rw/Rt) * (1/\emptyset_e{}^\wedge 2))}$$

The values of saturated hydrocarbon are calculated by the following equation.

$$Sh = 1 - Sw$$

Fig 3.7 is representing the relationship between water saturation (Sw) and hydrocarbons saturation (Sh) in the interested zone. The average value of Sw is 68.8% and Sh is 31.2% with overall trend showing low value of saturated hydrocarbons (Sh) in the interested zone.

Figure 3.7. Relationship of water and hydrocarbon saturation in Lockhart Formation

1) Indonesian equation

$$S_w = \left\{ \left[\left(\frac{Vsh^{2-V_{sh}}}{R_{sh}} \right)^{\frac{1}{2}} + \left(\frac{\emptyset_e^m}{R_w} \right)^{\frac{1}{2}} \right]^2 R_t \right\}^{-\frac{1}{n}}$$

The values of saturated hydrocarbon are calculated by the following equation.

$$Sh = 1 - Sw$$

Fig 3.8 is representing the relationship between (Sw) and (Sh) in interested zone. The average value of Sw is 63.8% and Sh is 36.2% with the overall trend showing low

28

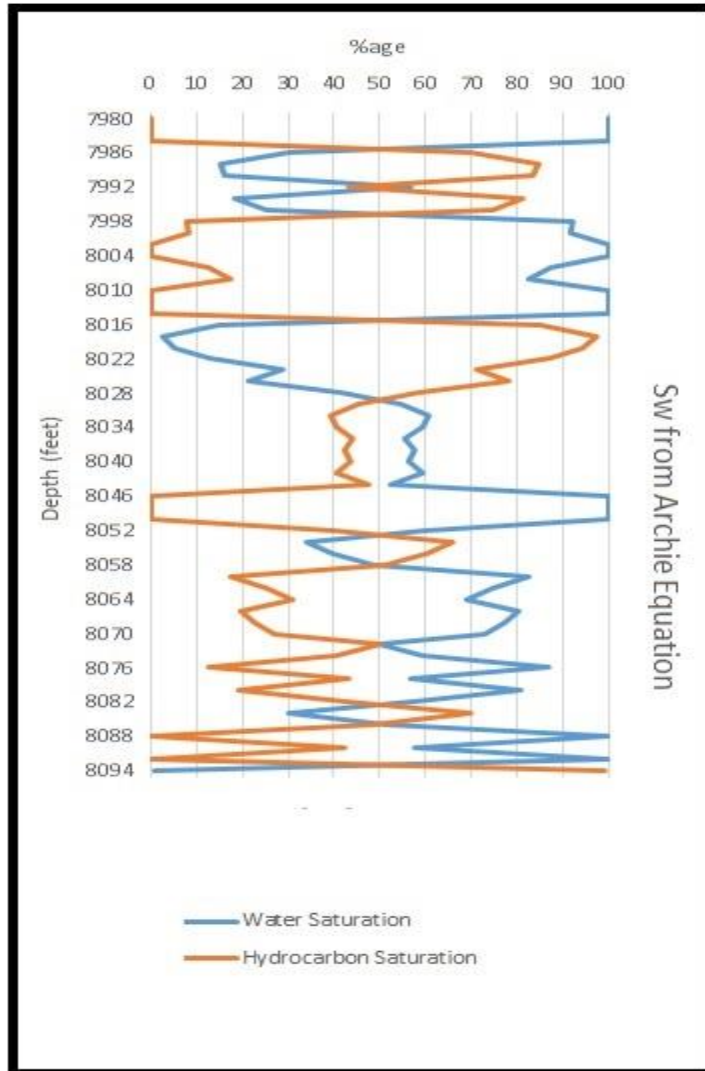value of the saturated hydrocarbon Sh in the interested zone.
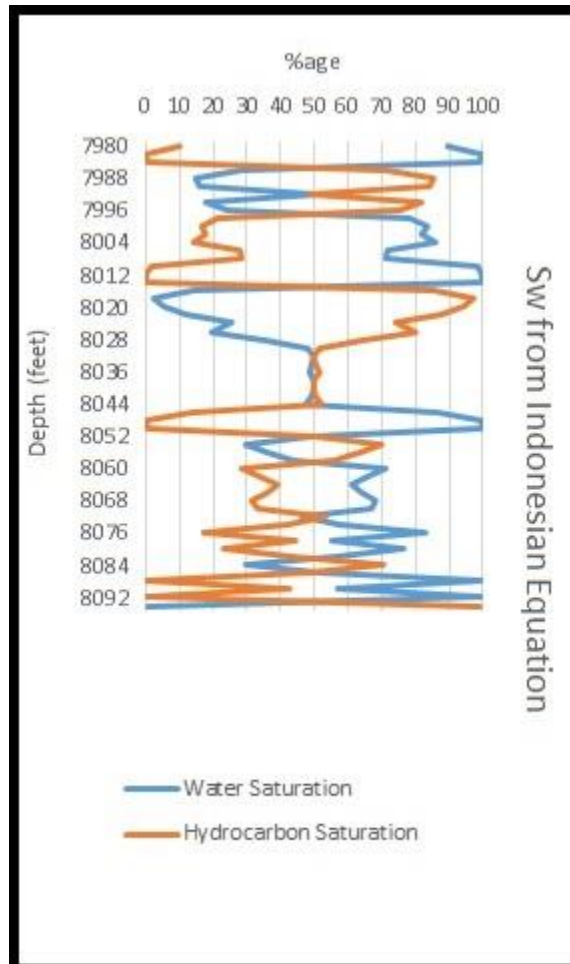
Figure 3.8. Relationship of water and hydrocarbon saturation in Lockhart Formation

3.4.2 Hangu Formation

In track-01 minimum CGR log value can be seen in this zone showing the presence of clay free lithology. The average CGR value was 11 API. The caliper log shows that hole is gauged throughout this zone.

In track-02 there is no such separation between LLD and LLS as shown in figure 3.2, but LLD values are low whereas the MSFL values are higher than the LLD values.

In track-03 there is no such neutron-density cross-overs can be seen. As neutron-density cross-overs formed where gas zone present and, in this zone, there is no gas present that is why no such neutron-density cross-overs can be seen.

3.4.2.1 Volume of shale (Vsh)

Figure 3.9 is representing the relationship between Vsh and Vclean in the zone of interest of Hangu Formation, showing fluctuating trend. Vsh and Vclean are showing mirror image of each other. Maximum value of Vsh is 19.5% observed at 8598 feet depth and minimum value of Vsh is zero observed at the depths of 8616 feet to 8634 feet. The average value of Vsh is 4.6%. Overall it is showing clean zone.
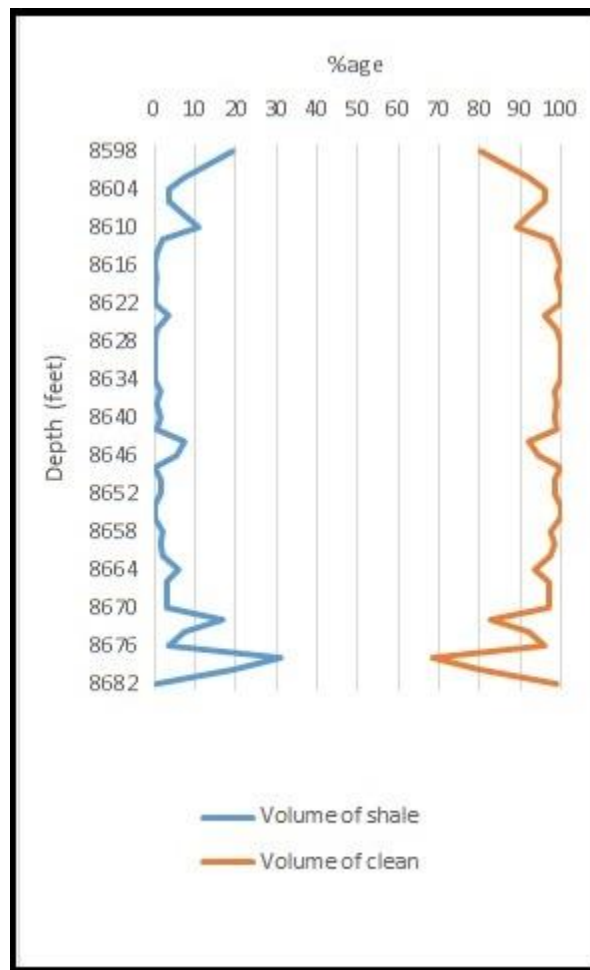
Figure 3.9. Volume of shale and volume of clean in Hangu Formation.

3.4.2.2 Average porosity

Hangu Formation is mainly composed of sandstone therefore use average porosity as there is no such rugosity observed in the zone. Calculation of average porosity can be calculated through neutron and density log. The porosity increases as Vsh increases in the zone. The average value of average porosity is 2.33%.
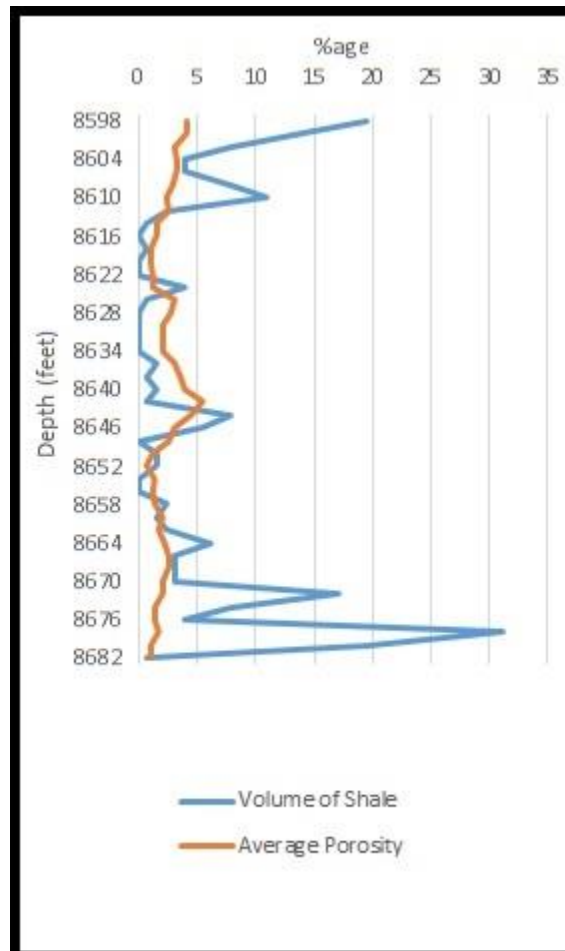
Figure 3.10. Volume of shale and average porosity in Hangu Formation.

3.4.2.3 Effective porosity

In very clean sands like Hangu Formation total porosity is equal to effective porosity. It represents pore space that contains hydrocarbon and non-clay water.

Figure 3.11 is representing the relationship between effective porosity and Vsh in the zone of interest. The average value of effective porosity this zone is 2.21%.

fi
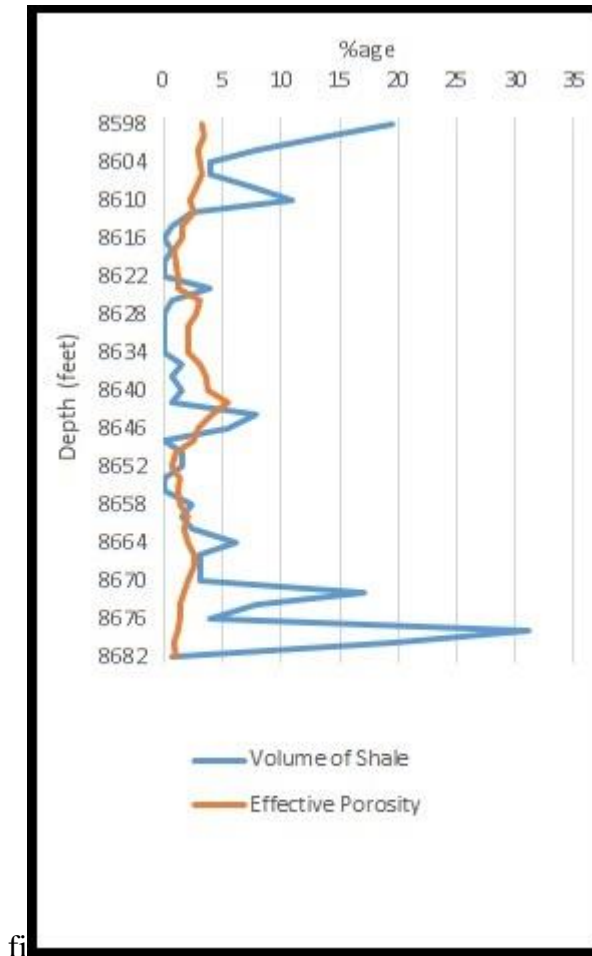
Figure 3.11. Volume of shale and effective porosity in Hangu Formation.

3.4.2.4 Relationship between average, effective porosity and volume of shale

Figure 3.12 is showing the relationship between sonic porosity, effective porosity and Vsh in the zone of interest. Where Vsh is low, the average porosity and effective porosity are equal. It is also evident from the figure that where, Vsh is high, the average porosity is greater than the effective porosity due to dirtiness of the lithology.
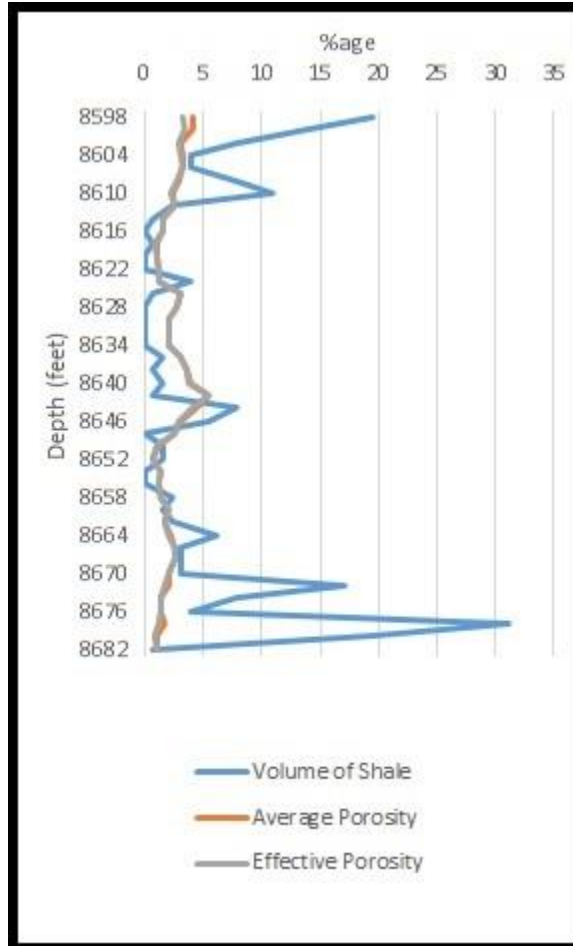
Figure 3.12. Relationship of volume of shale, average and effective porosity in Hangu Formation

3.4.2.5 Resistivity of Water

It is an acute parameter for the determination of water saturation. Rw calculate through Gen-9 and SP charts also Rw was computed using SP method equal to 0.018 ohm.m.

3.4.2.6 Saturation of water and hydrocarbons

During the log analysis of well study saturated water measured by the Archie Equation and Indonesian Equation.

1) Archie equation

Fig 3.13 is representing the relationship between the water saturation (Sw) and hydrocarbon saturation (Sh) in the interested zone. The average value of Sw is 89.2% and Sh is 10.8% in the zone of interest with overall trend showing low value of saturated hydrocarbons (Sh) in the interested zone.
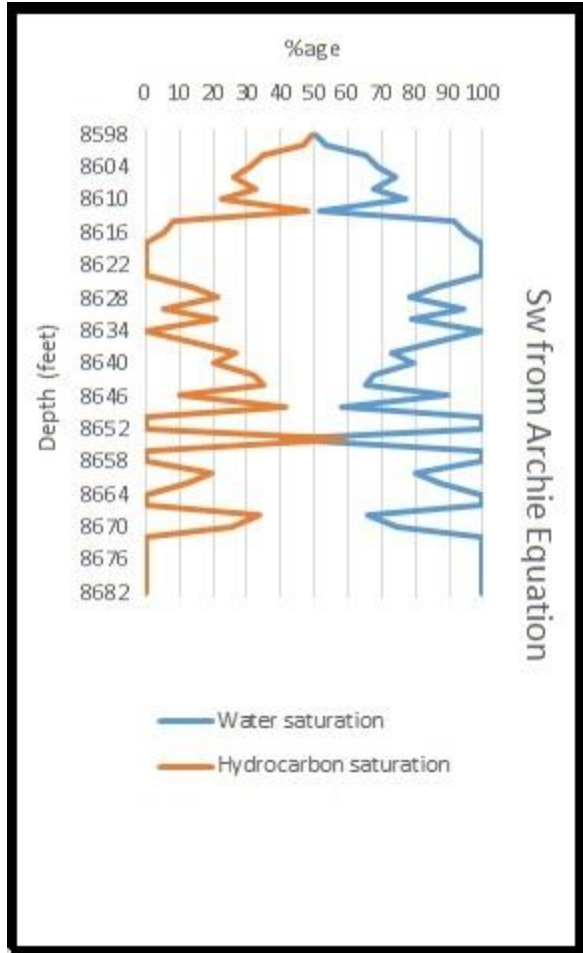
Figure 3.13. Relationship of water and hydrocarbon saturation in Hangu Formation

1) Indonesian equation

Fig 3.14 is representing the relationship between the water saturation (Sw) and hydrocarbon saturation (Sh) in the interested zone. The average value of Sw is 88% and Sh is 12% with overall trend showing low Sh in the zone of interest.
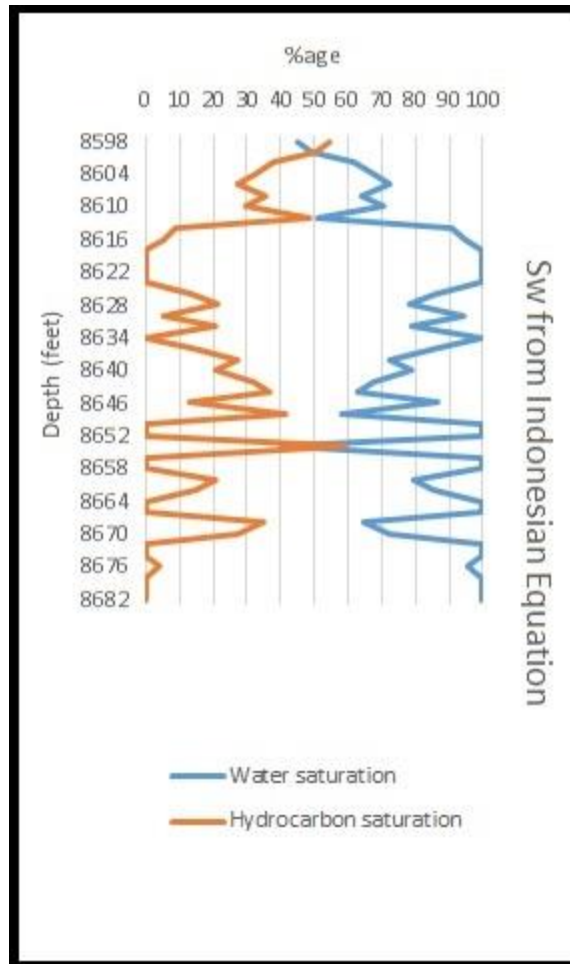
Figure 3.14. Relationship of water and hydrocarbon saturation in Hangu Formation

3.5   Results

Table 3.3 and Table 3.4 shows a comparison between various parameters calculated for the zone of interest in Lockhart Formation and Hangu Formation. Well logs of Tolanj-01 are not showing good hydrocarbon saturation. Average saturated hydrocarbon is 35% in the zone of Lockart Formation and 12% in the zone of Hangu Formation.

There is difference between the values of Sh and Sw while using Archie's and Indonesian equation because we use Archie for the clean lithology, whereas for dirty lithology we use Indonesian equation. Lockhart Formation is not clean that's why there is difference between the values of Sh and Sw for Archie's equation and Indonesian equation.

Table 3.3. Summary of petrophysical parameters of zone of interest in Lockhart Formation

Formation	Thickness (m)	Volume of shale (%)	Sonic porosity (%)	Effective porosity (%)	Saturation of hydrocarbon (%)
Lockhart	114	17.3	2.61	2.14	36.38

Table 3.4. Summary of petrophysical parameters of zone of interest in Hangu Formation

Formation	Thickness (m)	Volume of shale (%)	Average porosity (%)	Effective porosity (%)	Saturation of hydrocarbon (%)
Hangu	84	4.6	2.33	2.21	16.2

3.6   Identification of lithology and mineralogical composition

For the identification of lithological and mineralogical composition different cross plot were used like M-N, Neutron-density and Neutron-sonic cross plot.

3.6.1   Lockhart Formation

3.6.1.1 M-N cross plot

This cross plot is used for minerals identification. Two variables M on y-axis and N on x-axis are used. This cross plot may be used to help identify mineral mixtures from sonic, density and neutron logs (The CNL neutron log is used in the plot; the time average sonic response is assumed). Except in gas bearing formations, M and N are practically independent of porosity. They are defined as:

$$M = (tf - t) / (\rho b - \rho f) * 0.01$$

$$21N = ((\varphi N)f - \varphi N) / (\rho b - \rho f)$$

Points for binary mixtures plot along a line connecting the two mineral points. Ternary mixtures plot within the triangle defined by the three constituent minerals. The effect of gas, shaliness, etc. is to shift data points in the directions shown by the arrows (Schlumberger, 1997). The dolomite and sandstone lines on plot are divided by porosity

37

range as follows:

1) $\varphi = 0$ (tight formation)

2) $\varphi = 0$ to 12 p.u

3) $\varphi = 12$ to 27 p.u

4) $\varphi = 27$ to 40 p.u

Figure 3.15 is showing the M-N plot of Tolanj-01 well for Lockhart Formation. The marked values are making cluster, on the basis of cluster, circle is marked. M and N values lie in calcite region which verifies the lithology as limestone.

Figure 3.15. M-N cross plot for minerals identification (Schlumberger log interpretation charts, 1997).

3.6.1.2 Neutron-density cross plot

This cross plot is used for lithology identification. Bulk density values plotted on y-axis and values of neutron are plotted on x-axis. Neutron and density log values lie in calcite region, which verifies the lithology as limestone.

Figure 3.16. Neutron-density cross plot for lithology and minerals identification for Lockhart Formation (Schlumberger log interpretation charts, 1997).

3.6.1.3 Neutron-sonic cross plot

This cross plot is used for lithology identification. Sonic log values are plotted on y-axis and neutron log values are plotted on x-axis.

Figure 3.17 is showing the neutron-sonic cross plot of Tolanj-01 well. Neutron and sonic log values lie in calcite, which verifies the lithology as limestone.

Figure 3.17. Neutron-sonic cross plot for lithology and minerals identification for Lockhart Formation (Schlumberger log interpretation charts, 1997).

3.6.1.4 PEF log

It is litho-density log used for the determination of lithology by using density. The PEF log is mainly controlled by the mean atomic number of the formation. The PEF log is sensitive to differences in the mean atomic number of a formation without being sensitive

to changes in the porosity and fluid saturation of that lithology. This combination makes the PEF log an extremely good indicator of lithology. Higher value of atomic number shows that the lithology is less porous and denser. Therefore, higher Pe value shows that heavy minerals are present which indicates denser lithology.

Pe value for calcite minerals is 5.08 and in the Lockhart Formation there are variations in the values ranges from 5.2 to 6.4 and there is one peak observed which have value 9 to 13. These values show that Lockhart Formation is not pure and some other minerals are also present like sylvite, biotite limonite etc.

Figure 3.18. Photo electric factor-porosity cross plot for lithology and minerals identification for Lockhart Formation (Schlumberger log interpretation charts, 1997).

3.6.2   Hangu Formation

3.6.2.1 M-N cross plot

The marked values in figure 3.19 are making cluster, on the basis of cluster, circle is marked. M and N values lie in sandstone region which verifies the lithology as sandstone.
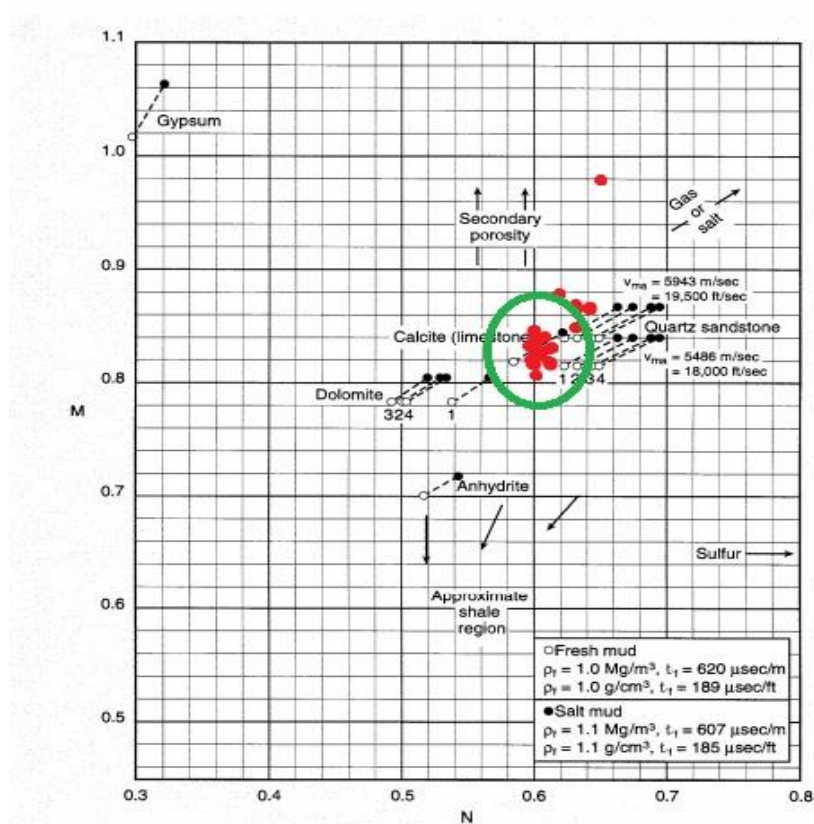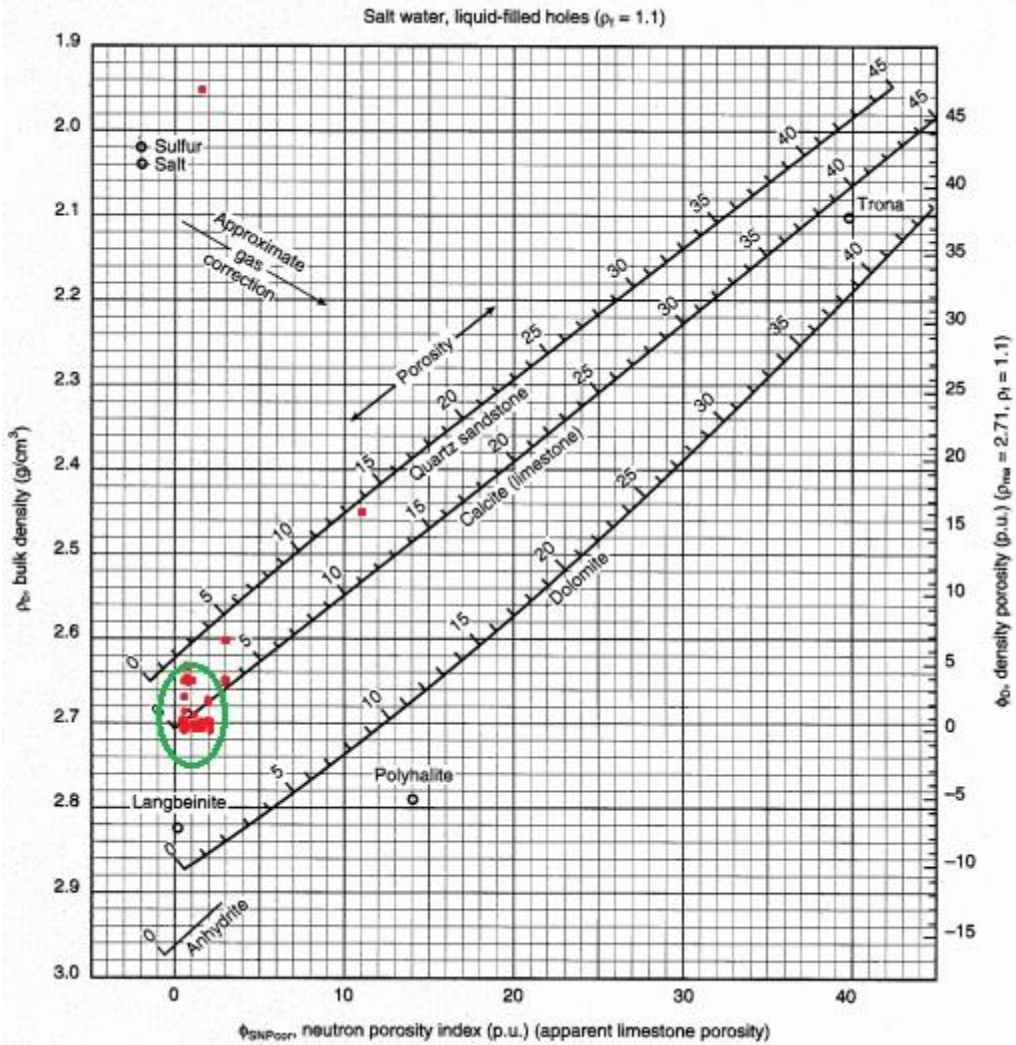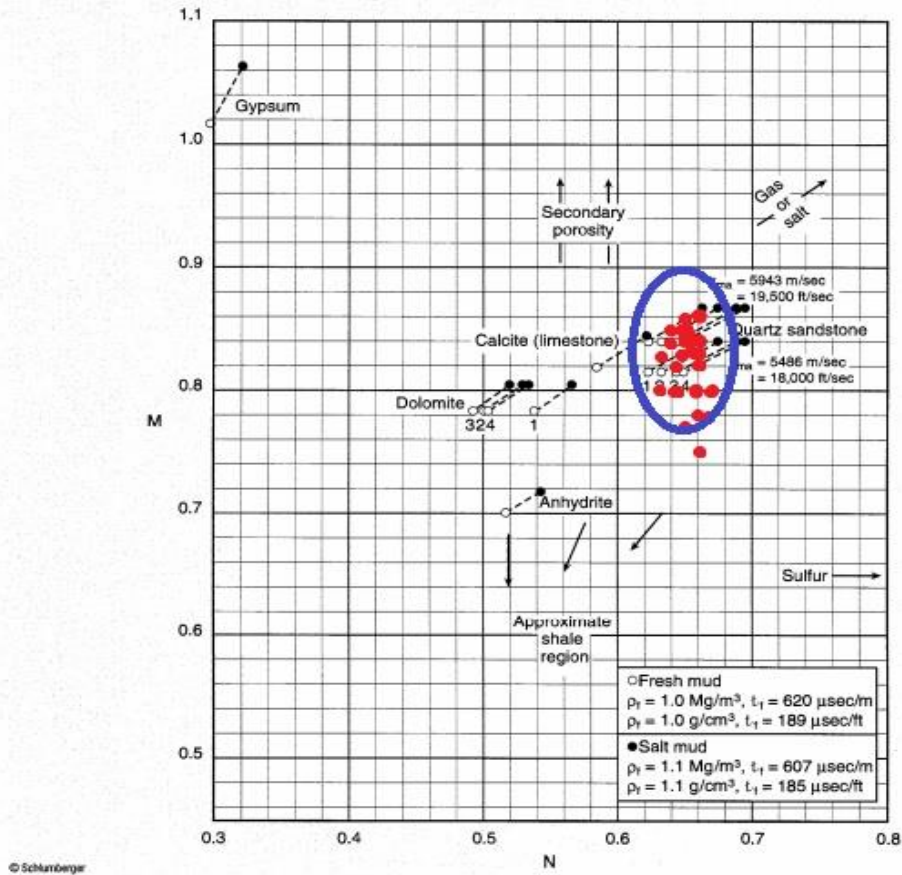

Figure 3.19. M-N cross plot for minerals identification (Schlumberger log interpretation charts, 1997).

3.6.2.2 Neutron-density cross plot

Figure 3.19 is showing the neutron-density cross plot of Tolanj-01 well. Neutron and density log values lie in sandstone region, which verifies the lithology as sandstone.
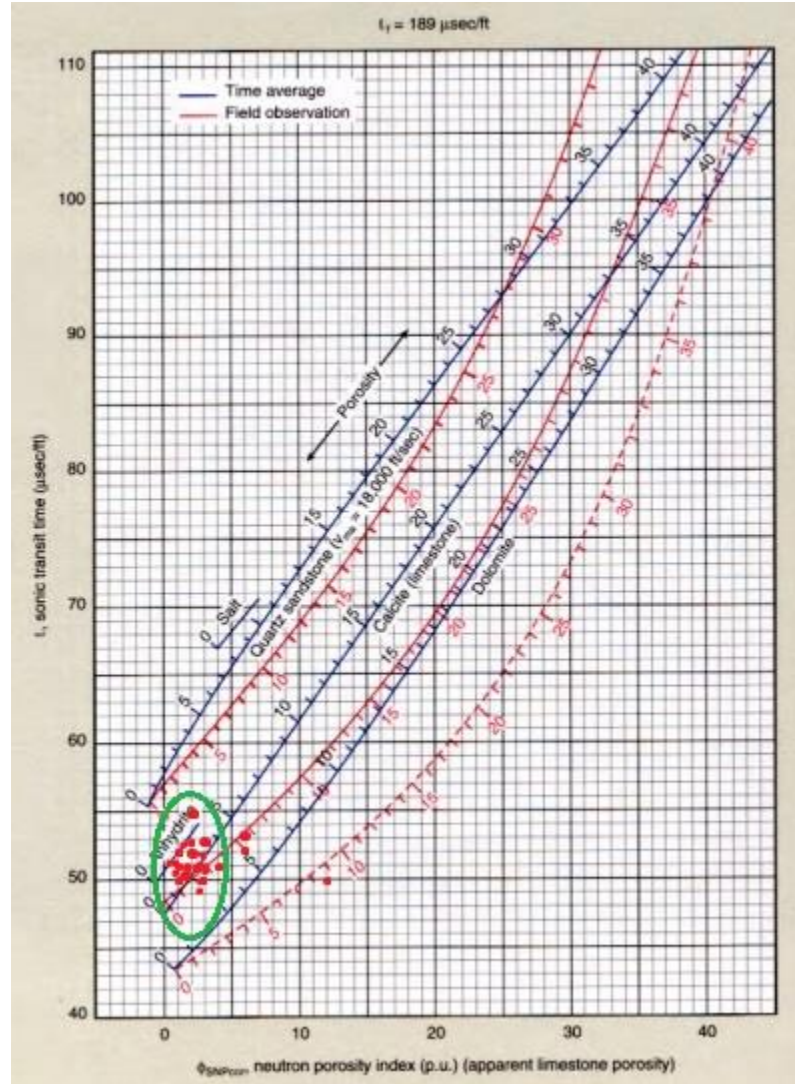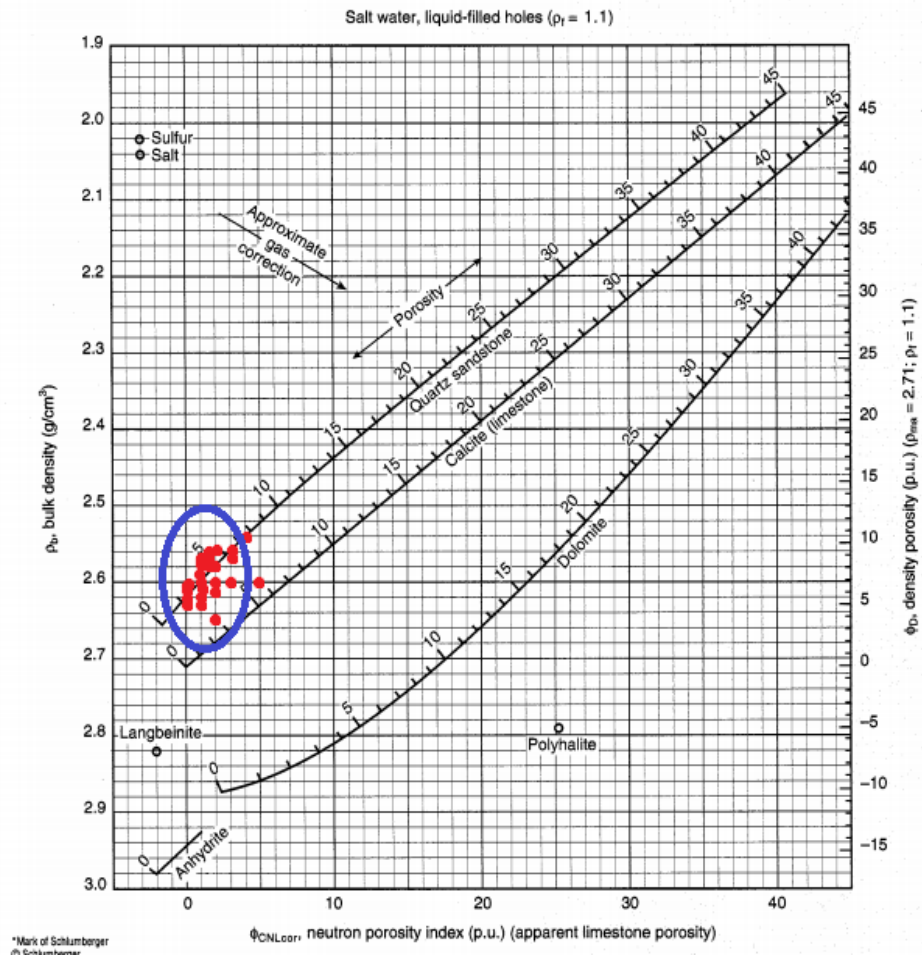
Figure 3.20. Neutron-density cross plot for lithology and minerals identification for Hangu Formation (Schlumberger log interpretation charts, 1997).

3.6.2.3 Neutron-sonic cross plot

Figure 3.20 is showing the neutron-sonic cross plot of Tolanj-01 well. Neutron and sonic log values lie in sandstone, which verifies the lithology as sandstone.
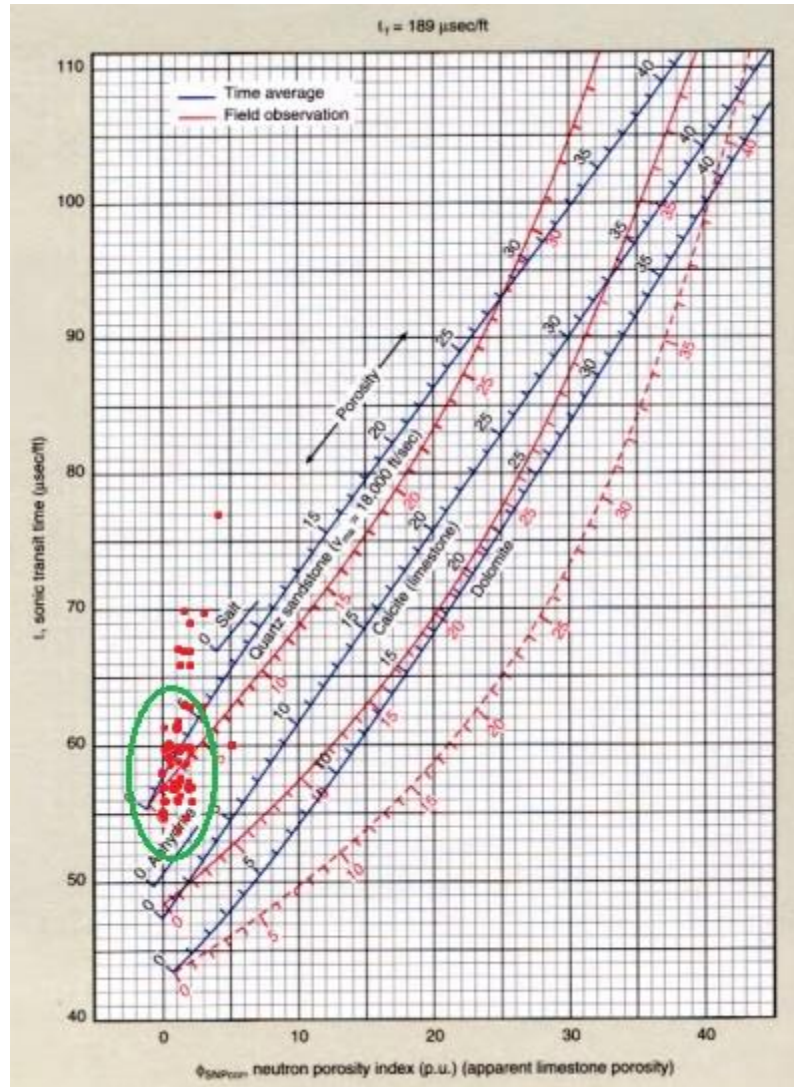
Figure 3.21. Neutron-sonic cross plot for lithology and minerals identification for Hangu Formation (Schlumberger log interpretation charts, 1997).

3.6.2.4 PEF log

Pe value for quartz minerals is 1.86 and in the Hangu Formation. There are variations in the values ranges from 2.1 to 3. These values show that Hangu Formation is not pure and some other minerals are also present like mica and muscovite.
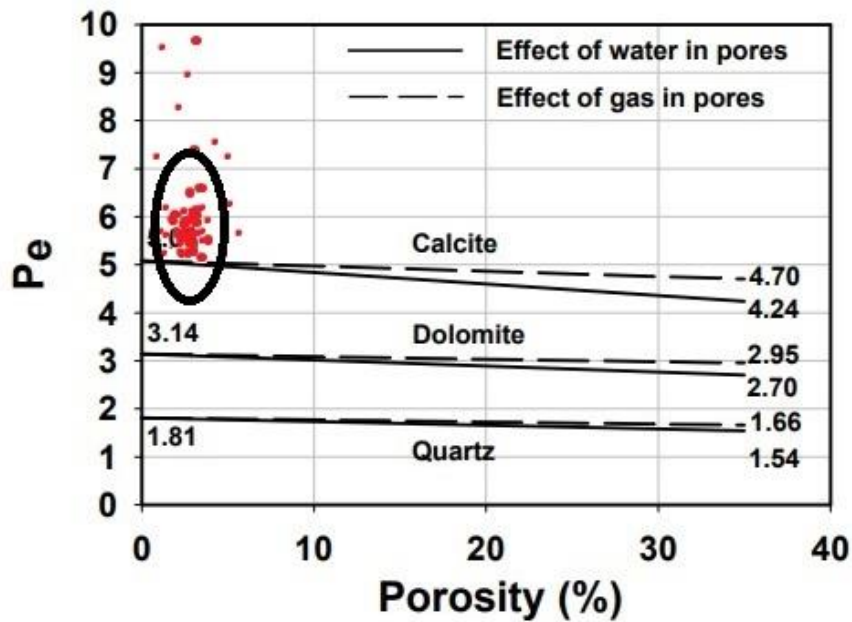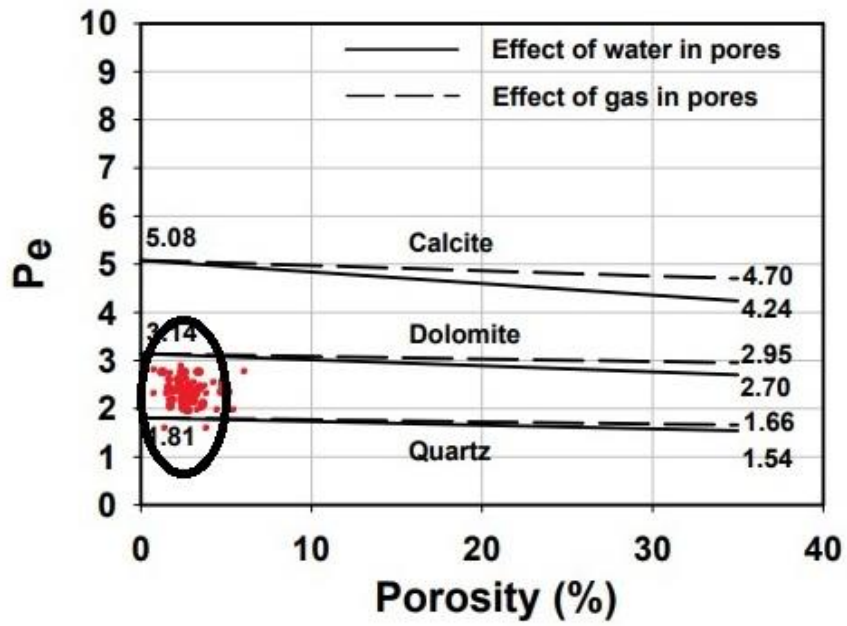
Figure 3.22. Photoelectric factor-porosity cross plot for lithology and minerals identification for Hangu Formation (Schlumberger log interpretation charts, 1997).

CONCLUSIONS

(1)   On the basis of petrophysical parameters, one prospect zone had been marked both in Lockhart Formation and Hangu Formation.

(2)   The zone in Lockhart Formation exhibited 17.3% volume of shale, 2.6% sonic porosity, 2.14% effective porosity and 36.38% hydrocarbon saturation. The zone in Hangu Formation exhibited 4.6% volume of shale, 2.33% average porosity, 2.21% effective porosity and 16.2% hydrocarbon saturation. In Lockhart Formation, neutron-density, neutron-sonic, PEF and M-N cross verified the lithology as limestone. In Hangu Formation, neutron-density, neutron-sonic, PEF and M-N cross verified the lithology as sandstone.

(3)   The petrophysical parameters elucidated the low hydrocarbons potential in Tolanj-01 well.

REFERENCES

Alger, R. P., 1980. Geological use of wireline logs in Developments in Petroleum Geology– 2, G.D. Hobson, Applied Science Publication, and London.

Bender, F. K., and Raza, H. A., 1989. Geology of Pakistan, with 140 figs., 38 tabs. Borntraeger, Berlin, Stuttgart.

Davies, L.M., 1930. Bibliography of Phanerozoic palaeontology and stratigraphy of Pakistan. Notes on the geology of Kohat. Asiatic Society of Bengal, Journal and Proceedings, New Series, 20, 207-224.

Eames, H. G., 1952. Bibliography of Phanerozoic palaeontology and stratigraphy of Pakistan, Macquarie University 2109, Australia.

Fatmi, A.N., 1977. Lithostratigraphic units of Kohat-Potwar Province, Indus Basin, Pakistan, GSP Memoirs, 10, 80.

Gee, E.R., 1989. Overview of the geology and structure of the Salt Range, with observations on related areas of northern Pakistan, in Malinconico, L.L., Jr., and Lillie, R.J., eds., Tectonics of the western Himalayas: Geological Society of America Special Paper 232, 95–111.

Jaswal, T. M., 1997. Structure and evolution of northern Potwar deformed zone, Pakistan.

Jaswal, T.M., Lillie, R. J., and Lawrence, R. D., 1997. Structure and Evolution of the Northern Potwar Deformed Zone, Pakistan. AAPG Bulletin, 81 (2). 308- 328.

Kazmi, A.H., and Jan, M.Q., 1997, Geology & Tectonics of Pakistan.

Khan, A.M., Ahmed R., H.A. Raza., and A. Kemal, 1989. Geology of Petroleum in Kohat-Potwar depression, Pakistan, Bull. Amer. Assoc. Petrol. Geol.

Kadri, I. B., 1995. Petroleum Geology of Pakistan, Published by Pakistan Petroleum Limited, Ferozsons (pvt) limited.

Malkani, M.S., (2007a, 2008a). Revised stratigraphy of Indus Basin (Pakistan): Sea level changes. ISBN 978-5-4262-0073-9, 608 "Cretaceous Ecosystem in Asia" held in Russia

Levorsen, A., 1967. Geology of Petroleum, W. H. Freeman & Co., San Francisco.

Latif, M. A., 1969. Stratigraphy of south eastern Hazara and parts of Rawalpindi and Muzaffarabad districts of West Pakistan and Kashmir. Ph. D. thesis.

Meissner, Jr. C., Master, J.M., Rashid, M.A. and Hussain, M., 1974. Stratigraphy of the Kohat Quadrangle, Pakistan. Us. Geol. Surv. Prof. Paper, 716-D, p.1-30.

Raza, H. A., Ahmed, R., Ali, S. M., & Ahmad. J., 1989. Petroleum prospects Sulaiman Sub Basin, Pakistan. Pakistan Journal of Hydrocarbon Research.

Schlumberger log interpretation charts, 1997.

Shah, S. M. I., 1977. Stratigraphy of Pakistan, Memoirs of Geological survey of Pakistan.

Shah, S.M.I., 1977. Ahmed, R., Cheema, M.R., Fatmi, A.N., Iqbal, M.W.A., Raza, H.A., and Raza, S.M., 1989 and 1995. Stratigraphy of Pakistan: Geological Survey of Pakistan, Memoirs, V (12), 137.

APPENDICES

APPENDIX-A

Zone in Lockhart Formation

D (ft.)	Vsh %	Vclean %	PHIA %	PHIE %	Rw ohm.m	Sw (A) %	Sh (A) %	Sw (I) %	Sh (I) %	PEF
7980	16.39	83.60	0.5	0.42	0.023	100	0	100	0	5.8
7982	18.03	81.96	0.5	0.41	0.023	100	0	100	0	5.3
7984	21.31	78.68	0.5	0.39	0.023	100	0	100	0	5.5
7986	14.75	85.24	1.742	1.48	0.023	36.10	63.89	33.75	66.24	6.7
7988	19.67	80.32	3.23	2.59	0.023	18.45	81.54	17.51	82.48	7.8
7990	14.75	85.24	2.86	2.44	0.023	19.64	80.35	18.84	81.15	7.8
7992	13.11	86.88	0.81	0.70	0.023	68.09	31.90	60.28	39.71	7
7994	13.11	86.88	2.36	2.05	0.023	22.26	77.73	21.32	78.67	7.2
7996	9.83	90.16	1.74	1.57	0.023	30.53	69.47	29.27	70.72	7
7998	13.11	86.88	0.5	0.43	0.023	100	0	91.22	8.77	6.8
8000	8.19	91.80	0.5	0.45	0.023	100	0	98.28	1.71	6
8002	16.39	83.60	0.5	0.42	0.023	100	0	94.69	5.30	6
8004	21.31	78.68	0.5	0.39	0.023	100	0	98.11	1.88	6.4
8006	21.31	78.68	0.75	0.59	0.023	100	0	83.30	16.69	6
8008	16.39	83.60	0.75	0.62	0.023	98.73	1.26	83.34	16.65	5.9
8010	24.59	75.40	0.5	0.37	0.023	100	0	100	0	5.5
8012	21.31	78.68	0.5	0.39	0.023	100	0	100	0	5.7
8014	21.31	78.68	0.5	0.39	0.023	100	0	100	0	6
8016	21.31	78.68	4.86	3.82	0.023	17.72	82.27	17.04	82.95	9
8018	16.39	83.60	25.10	20.98	0.023	3.23	96.76	3.21	96.78	13
8020	32.78	67.21	14.07	9.45	0.023	6.54	93.45	6.38	93.62	10
8022	37.70	62.29	6.41	3.99	0.023	15.23	84.76	14.25	85.74	6
8024	32.78	67.21	2.31	1.55	0.023	34.52	65.47	29.90	70.09	5.8
8026	29.50	70.49	2.93	2.06	0.023	25.94	74.05	23.49	76.50	6
8028	27.86	72.13	1.5	1.08	0.023	49.55	50.44	41.73	58.26	5.4
8030	18.03	81.96	1	0.81	0.023	65.41	34.58	56.56	43.43	5.2
8032	26.22	73.77	1	0.73	0.023	72.68	27.31	57.77	42.22	5.8
8034	24.59	75.40	1	0.75	0.023	71.10	28.89	57.52	42.47	5.7
8036	19.67	80.32	1	0.80	0.023	66.75	33.24	56.80	43.19	5.8
8038	19.67	80.32	1	0.80	0.023	68.93	31.06	58.67	41.32	5.5
8040	18.03	81.96	1	0.81	0.023	67.56	32.49	58.42	41.57	5.4
8042	24.59	75.40	1	0.75	0.023	71.10	28.89	57.52	42.47	6
8044	14.75	85.24	1	0.85	0.023	62.89	37.10	56.08	43.91	5.7
8046	18.03	81.96	0.5	0.40	0.023	100	0	99.66	0.34	5.8
8048	16.39	83.60	0.5	0.41	0.023	100	0	100	0	5.6
8050	19.67	80.32	0.5	0.40	0.023	100	0	100	0	5.8
8052	31.14	68.85	1.31	0.90	0.023	71.66	28.33	57.23	42.76	5.9
8054	34.42	65.57	2.31	1.51	0.023	40.86	59.13	35.03	64.97	5.4
8056	19.67	80.32	1.5	1.20	0.023	47.57	52.42	42.60	57.39	5.7
8058	19.67	80.32	1.31	1.05	0.023	58.81	41.18	51.88	48.11	5.2

8060	16.39	83.60	0.75	0.62	0.023	98.73	1.26	83.34	16.65	5.2
8062	14.75	85.24	0.75	0.63	0.023	89.65	10.34	77.16	22.83	5.4
8064	18.03	81.96	1	0.81	0.023	82.74	17.25	71.55	28.44	5.6
8066	29.50	70.49	1	0.70	0.023	96.21	3.78	73.71	26.28	5.6
8068	18.03	81.96	1	0.81	0.023	92.51	7.48	80.01	19.99	5.8
8070	13.11	86.88	1	0.86	0.023	87.27	12.72	78.97	21.02	6
8072	13.11	86.88	1.31	1.13	0.023	59.56	40.43	55.14	44.85	5.4
8074	4.918	95.08	1	0.95	0.023	71.33	28.66	68.99	31.01	6
8076	8.196	91.80	1	0.91	0.023	100	0	98.54	1.45	5.9
8078	4.918	95.08	1	0.95	0.023	68.01	31.98	65.78	34.21	6.4
8080	6.55	93.44	0.75	0.70	0.023	96.77	3.22	91.10	8.89	6
8082	3.27	96.72	1	0.96	0.023	68.76	31.23	67.29	32.70	5.9
8084	4.91	95.08	1.81	1.72	0.023	35.96	64.03	35.30	64.69	6.3
8086	0	100	1	1	0.023	61.91	38.08	61.91	38.08	5.8
8088	0	100	0.5	0.5	0.023	100	0	100	0	5.5
8090	1.63	98.36	1	0.98	0.023	68.95	31.04	68.23	31.76	5.6
8092	13.11	86.88	0.75	0.65	0.023	100	0	100	0	6
8094	6.53	93.44	100	93.44	0.023	0.93	99.06	0.93	99.06	6

Zone in Hangu Formation

D	Vsh	Vclean	PHIA	PHIE	Rw	Sw	Sh	Sw	Sh	PEF
(ft.)	%	%	%	%	ohm.m	(A)	(A)	(I)	(I)	
						%	%	%	%	
8598	19.53	80.46	4.11	3.30	0.018	57.32	42.67	50.67	49.32	2.3
8600	14.06	85.93	4.08	3.50	0.018	60.49	39.50	55.63	44.36	2.2
8602	7.81	92.18	3.11	2.86	0.018	73.92	26.07	69.93	30.06	2.6
8604	3.91	96.09	3.25	3.13	0.018	78.23	21.76	76.31	23.68	2.2
8606	3.91	96.09	3.33	3.20	0.018	83.83	16.16	81.81	18.18	2.3
8608	7.82	92.18	3.01	2.77	0.018	76.49	23.50	72.23	27.76	2.3
8610	10.93	89.06	2.43	2.16	0.018	87.47	12.52	78.94	21.05	2.3
8612	2.34	97.65	2.61	2.55	0.018	58.78	41.21	57.73	42.26	2.1
8614	0.78	99.21	1.61	1.60	0.018	100	0	100	0	2.5
8616	0	100	1.61	1.61	0.018	100	0	100	0	2.3
8618	0.78	99.21	0.96	0.96	0.018	100	0	100	0	2.1
8620	0	100	0.96	0.96	0.018	100	0	100	0	2.4
8622	0	100	1.29	1.29	0.018	100	0	100	0	2.1
8624	3.90	96.09	1.29	1.23	0.018	100	0	100	0	2.5
8626	0.78	99.21	3.08	3.05	0.018	98.14	1.85	97.66	2.33	2.6
8628	0	100	2.75	2.75	0.018	88.81	11.18	88.81	11.18	2.3
8630	0	100	2.11	2.11	0.018	100	0	100	0	2
8632	0	100	2.11	2.11	0.018	89.79	10.20	89.79	10.20	2.8
8634	0	100	2.11	2.12	0.018	100	0	100	0	2.8
8636	1.56	98.43	3.08	3.03	0.018	98.92	1.07	97.93	2.06	2.1
8638	0.78	99.21	3.65	3.63	0.018	82.76	17.23	82.42	17.57	3
8640	1.56	98.43	3.90	3.84	0.018	90.15	9.84	89.44	10.55	2
8642	0.78	99.21	5.54	5.50	0.018	77.06	22.92	76.85	23.14	2.6
8644	7.81	92.18	4.41	4.05	0.018	73.90	26.09	71.03	28.96	2.1
8646	5.46	94.53	3.11	2.94	0.018	100	0	98.19	1.80	3
8648	0	100	2.61	2.62	0.018	66.28	33.72	66.28	33.71	2.3
8650	1.56	98.43	1.14	1.12	0.018	100	0	100	0	2.8
8652	1.56	98.43	0.64	0.63	0.018	100	0	100	0	2.1
8654	0	100	1.46	1.46	0.018	45.70	54.29	45.70	54.29	2.4
8656	0	100	1.14	1.145	0.018	100	0	100	0	2.1
8658	2.34	97.65	1.46	1.43	0.018	100	0	100	0	2.4
8660	1.56	98.43	2.11	2.07	0.018	91.22	8.77	89.90	10.09	2.3
8662	2.34	97.65	1.79	1.74	0.018	99.06	0.93	96.50	3.49	2.2
8664	6.25	93.7	2.29	2.14	0.018	100	0	100	0	2.4
8666	3.12	96.87	2.61	2.53	0.018	100	0	100	0	2.3
8668	3.12	96.87	2.61	2.53	0.018	74.95	25.04	73.14	26.85	2.3
8670	3.12	96.87	2.11	2.04	0.018	84.61	15.38	82.10	17.89	2.1
8672	17.18	82.81	2.11	1.74	0.018	100	0	100	0	2.4
8674	7.81	92.18	1.46	1.35	0.018	100	0	100	0	2.1
8676	3.906	96.09	1.46	1.41	0.018	100	0	100	0	2
8678	31.25	68.75	1.79	1.23	0.018	100	0	100	0	2.4
8680	19.53	80.46	1	0.8	0.018	100	0	100	0	3.2
8682	0.78	99.22	1	0.99	0.018	100	0	100	0	3

APPENDIX-B
Calculation of Rw for Lockhart Formation

The procedure for the calculation of Rw is as follows:

1. Calculation of Geothermal Gradient
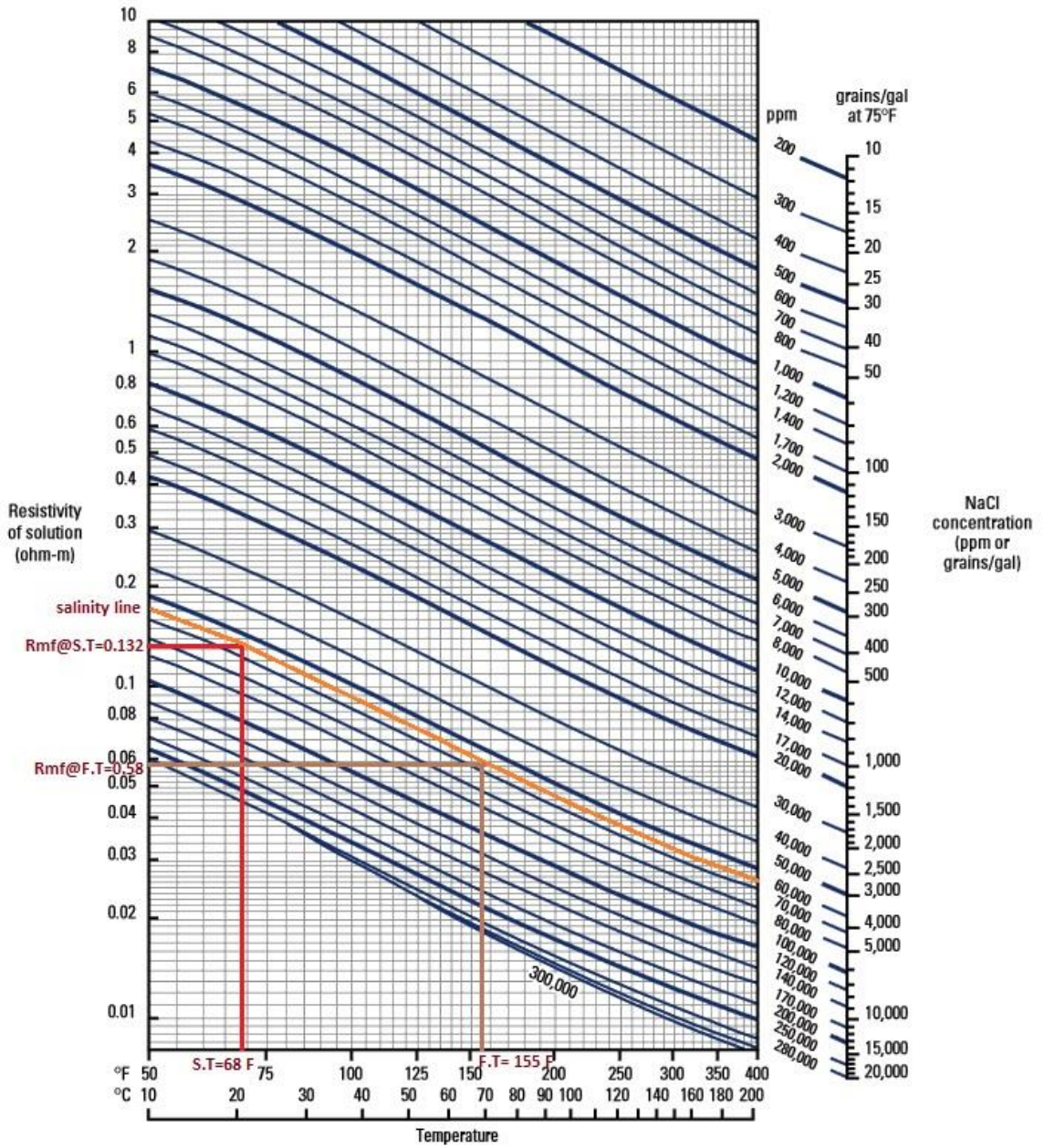
    Geothermal gradient = (Bottom hole temp – surface temp) / total depth
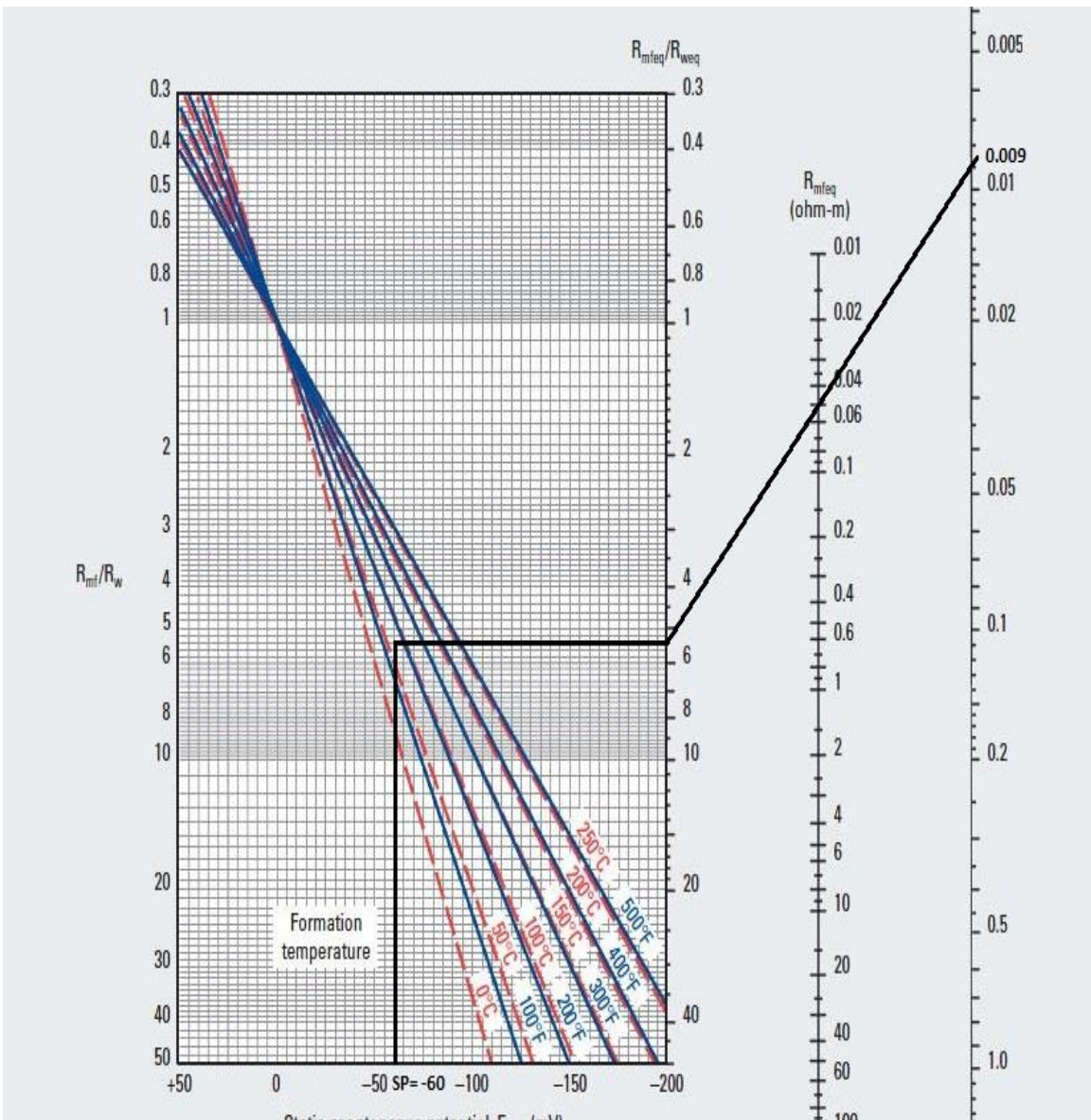
    = (179 °F - 68 °F) / 10167 ft

    = 0.0109 °F/ft

2. Calculation of formation Temperature = (Geothermal Gradient * Formation top) +
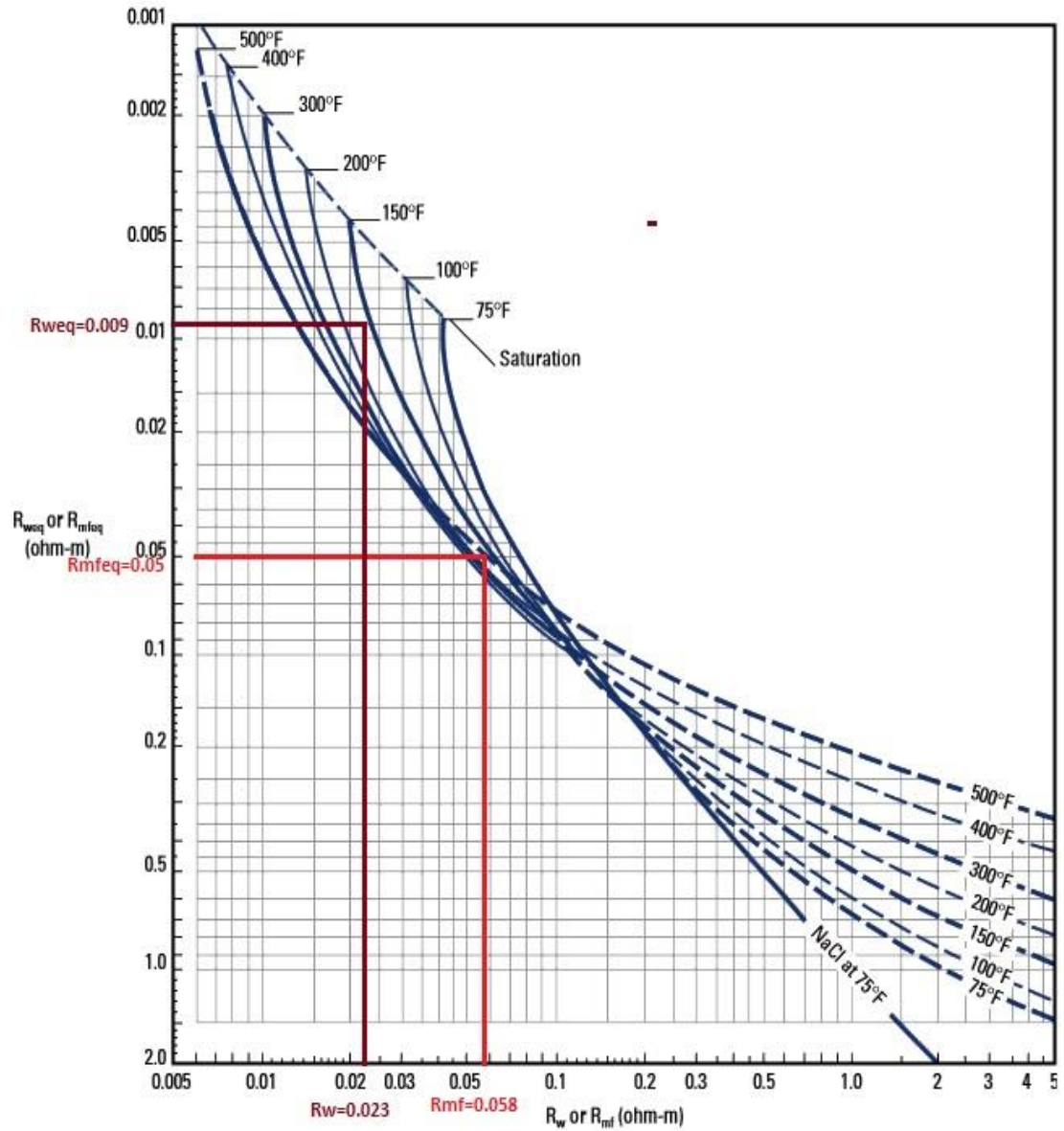
    Surface temperature

    = (0.0109*7979) + 68

    = 154.97 °F

3. Rmf @ formation temperature = 0.058 ohm.m   (from Gen-9 chart)

4. Convert Rmf to Rmfeq = 0.05 ohm.m   (from SP-2 chart)

5. Static spontaneous potential (SSP) = -60   (from SP log)

6. Convert Rmfeq to Rweq = 0.009 ohm.m   (from SP-1 chart)

7. Calculate Rw = 0.023 ohm.m   (from SP-2 chart)

Conversion approximated by $R_2 = R_1 [(T_1 + 6.77)/(T_2 + 6.77)]°F$ or $R_2 = R_1 [(T_1 + 21.5)/(T_2 + 21.5)]°C$

53

Bottom hole temperature	= 179 ˚F
Surface Temperature	= 68 ˚F
Total Depth	= 10167 ft.
Formation top	= 7979 ft.
Rmf @ surface temperature (68 ˚F)	= 0.132 ohm.m

Calculation of Rw for Hangu Formation

The procedure for the calculation of Rw is as follows:

1. Calculation of Geothermal Gradient

   Geothermal gradient = (Bottom hole temp – surface temp) / total depth

   = (179 °F - 68 °F) / 10167 ft

   = 0.0109 °F/ft

2. Calculation of formation Temperature = (Geothermal Gradient * Formation top) + Surface temperature

   = (0.0109*8391) + 68

   = 159.46 °F

3. Rmf @ formation temperature = 0.056 ohm.m   (from Gen-9 chart)

4. Convert Rmf to Rmfeq = 0.047 ohm.m   (from SP-2 chart)

5. Static spontaneous potential (SSP) = -78   (from SP log)

6. Convert Rmfeq to Rweq = 0.0058 ohm.m   (from SP-1 chart)

7. Calculate Rw = 0.018 ohm.m   (from SP-2 chart)

Conversion approximated by $R_2 = R_1 [(T_1 + 6.77)/(T_2 + 6.77)]°F$ or $R_2 = R_1 [(T_1 + 21.5)/(T_2 + 21.5)]°C$

57
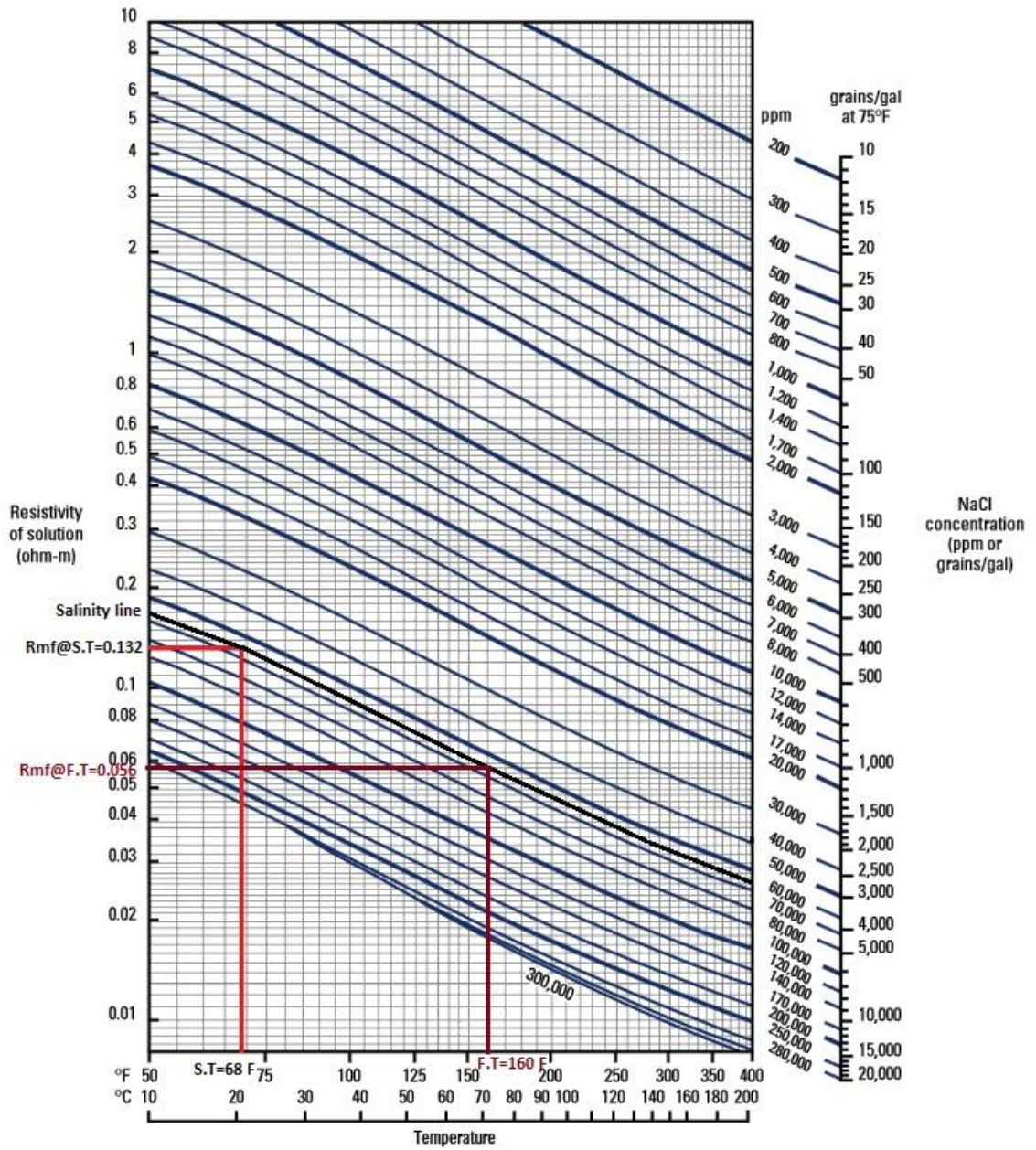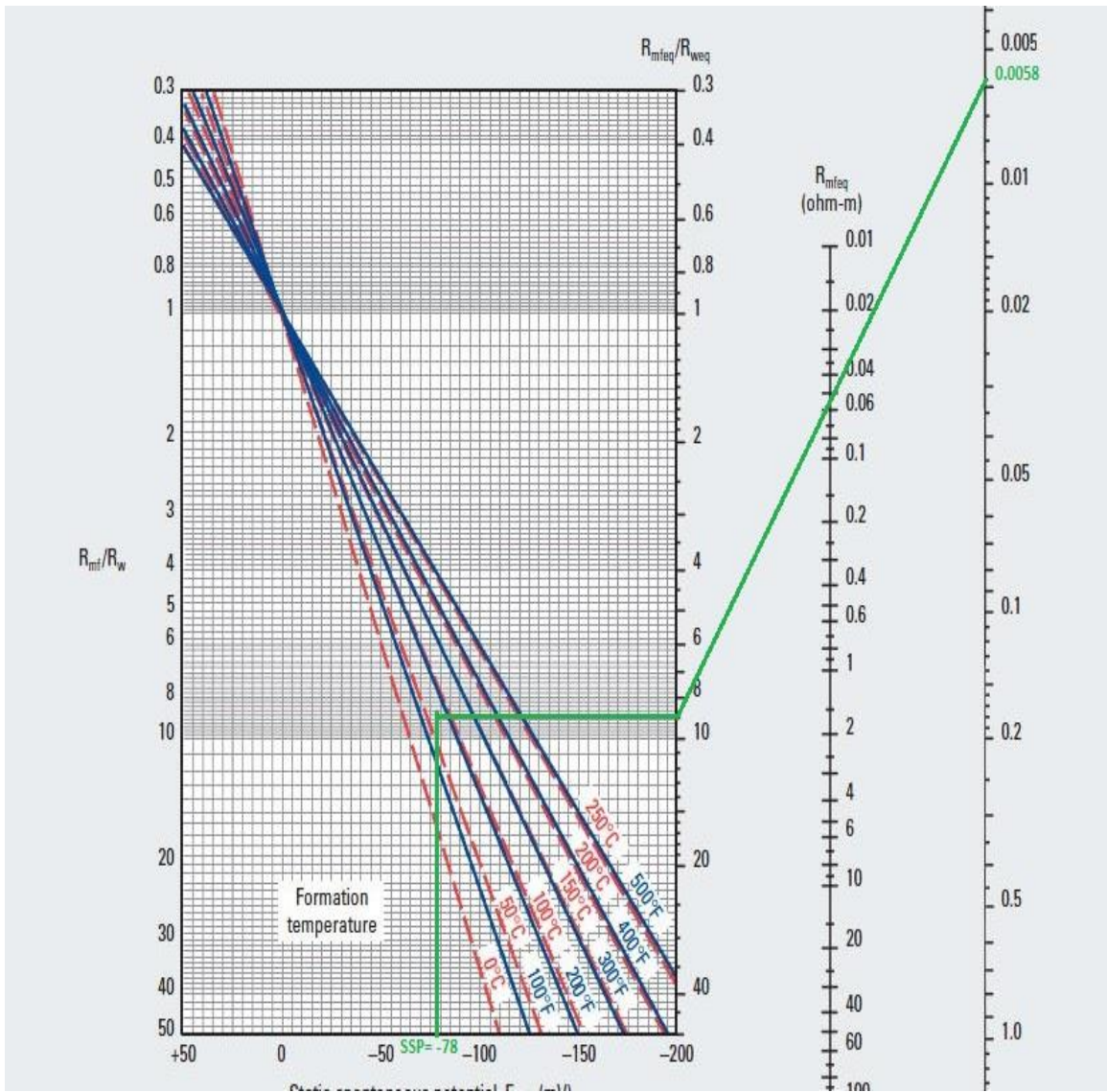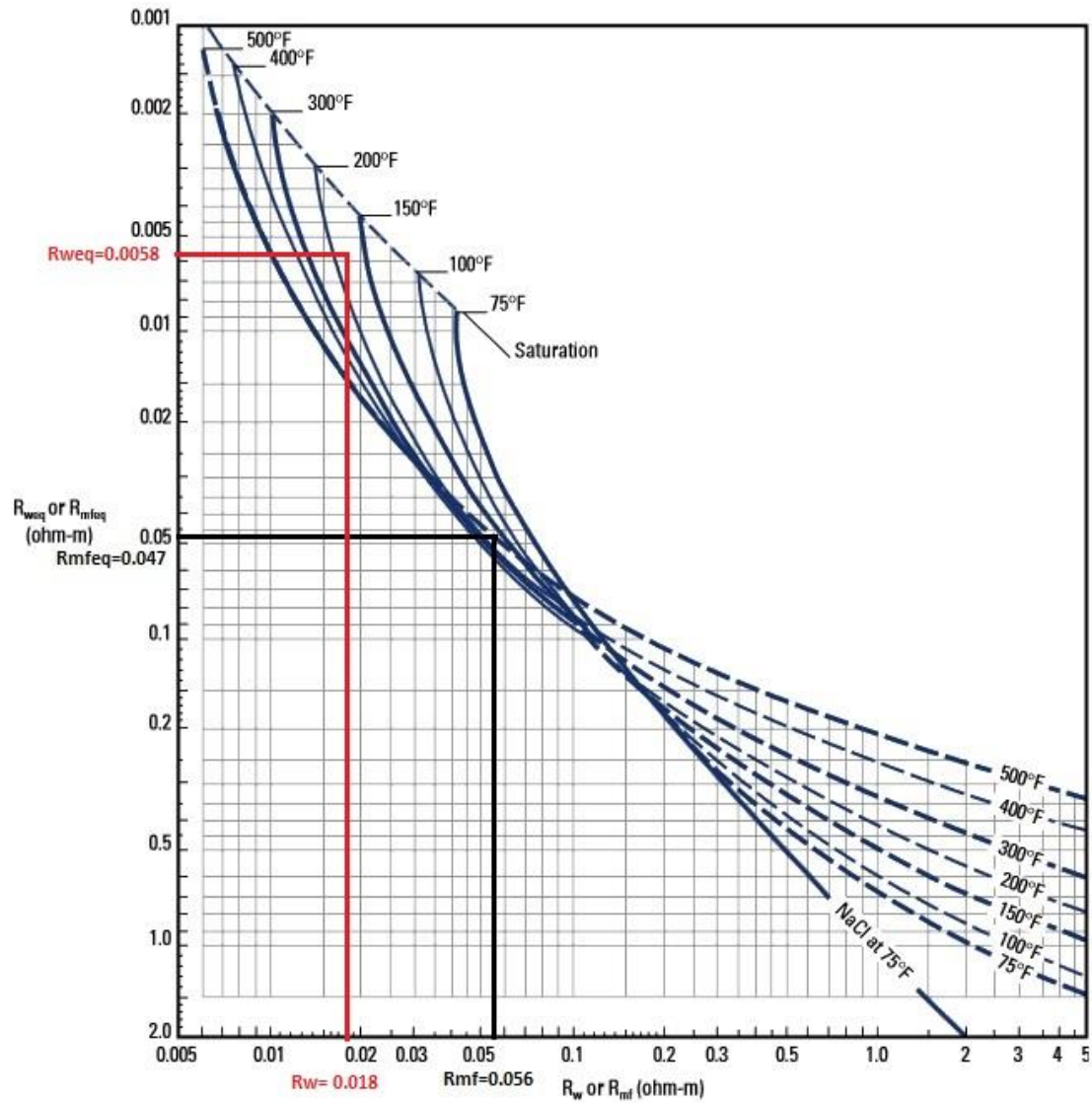
Bottom hole temperature	= 179 ˚F	
Surface Temperature	= 68 ˚F	
Total Depth	= 10167 ft.	
Formation top	= 8391 ft.	
Rmf @ surface temperature (68 ˚F)	= 0.132 ohm.m	

PETROPHYSICAL ANALYSIS OF TOLANJ-01 WELL, KHUSHALGARH BLOCK A, UPPER INDUS BASIN, PAKISTAN

BY

ABDUL AHAD, ABDUL HAMEED, MUHAMMAD MUNHIM-UR-REHMAN

PETROPHYSICAL ANALYSIS OF TOLANJ-01 WELL, KHUSHALGARH BLOCK A, UPPER INDUS BASIN, PAKISTAN